

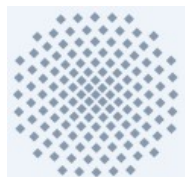


Dipartimento di Ingegneria Civile, Ambientale e Meccanica  
Università degli Studi di Trento

# An Introduction to Smooth Particle Hydrodynamics (SPH) for Free Surface Flows

**Prof. Dr.-Ing. Michael Dumbser**

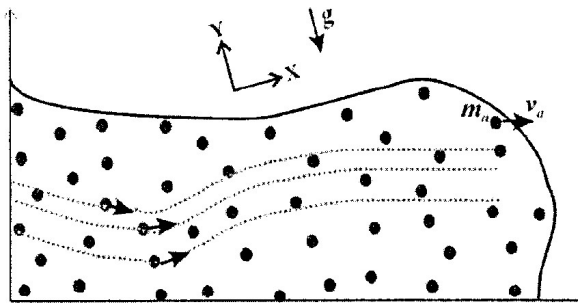
Dr.-Ing. A. Ferrari, Prof. E.F. Toro, Prof. A. Armanini



**HLRS**  
Institut für Wasserbau und Wassermengenwirtschaft  
Universität Stuttgart

# Fundamental Aspects

The continuum fluid is discretized by a finite set of discrete values defined at observation points, the so-called **particles**, which move with the material velocity of the continuum.



[M. X. Rodriguez-Paz, J. Bonet,  
2003]

From the *mathematical* point of view, the particles are *interpolation points*.

From the *physical* point of view, they are *material particles* with associated properties, like mass, position, velocity and density.



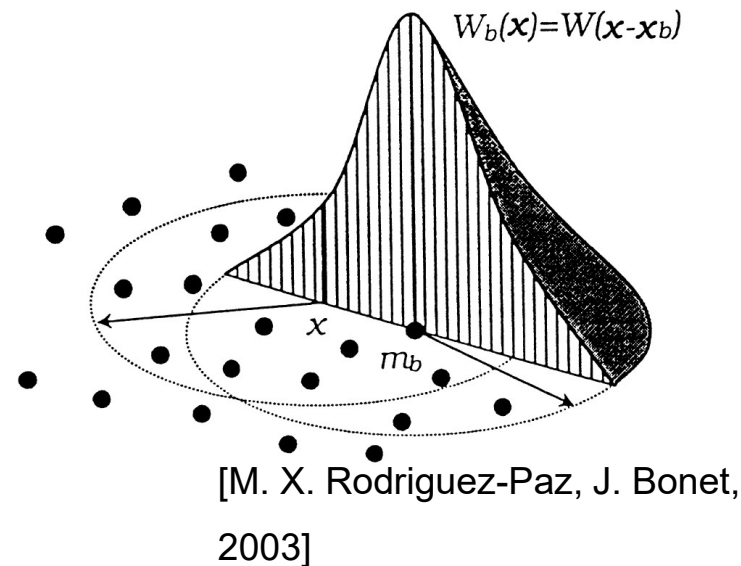
*It resembles a molecular dynamics system.*

# Fundamental Aspects

The SPH interpolation of the value of a function  $f(\mathbf{x})$  and its gradient  $\nabla f(\mathbf{x})$ , at a point  $\mathbf{x}$  are evaluated in terms of a ***local interpolating kernel function***  $W(\mathbf{x} - \mathbf{x}', l)$  and  $\nabla W(\mathbf{x} - \mathbf{x}', l)$ :

$$f(\mathbf{x}) = \int_{\Omega} f(\mathbf{x}') W(\mathbf{x} - \mathbf{x}', l) d\mathbf{x}'$$

$$\nabla f(\mathbf{x}) = \int_{\Omega} f(\mathbf{x}') \nabla W(\mathbf{x} - \mathbf{x}', l) d\mathbf{x}'$$



where  $l$  is the ***smoothing length***, which determines the support of the kernel function.

To obtain the estimate of the gradient  $\nabla f(\mathbf{x})$ , the integration by parts has been used and the residual boundary terms have been neglected.

# Fundamental Aspects

$$f(\mathbf{x}) = \int_{\Omega} f(\mathbf{x}') W(\mathbf{x} - \mathbf{x}', l) d\mathbf{x}' \quad \nabla f(\mathbf{x}) = \int_{\Omega} f(\mathbf{x}') \nabla W(\mathbf{x} - \mathbf{x}', l) d\mathbf{x}'$$

The kernel function  $W$  is defined such that:

- The kernel  $W$  is a smooth, differentiable function and mimics the *Dirac  $\delta$ -function* in the limit  $l \rightarrow 0$ .
- It must reproduce exactly a constant function  $f(\mathbf{x})$  and therefore satisfy:

$$\int_{\Omega} W(\mathbf{x} - \mathbf{x}', l) d\mathbf{x}' = 1$$

$$\int_{\Omega} \nabla W(\mathbf{x} - \mathbf{x}', l) d\mathbf{x}' = 0$$



***The consistency conditions***

- The kernel is *symmetric* and its gradient antisymmetric:

$$W(\mathbf{x} - \mathbf{x}', l) = W(\mathbf{x}' - \mathbf{x}, l)$$

$$\nabla W(\mathbf{x} - \mathbf{x}', l) = -\nabla W(\mathbf{x}' - \mathbf{x}, l)$$

# Fundamental Aspects

The most widely applied in the SPH simulations are:

- The ***truncated Gaussian distribution***

$$W_G(q, l) = \left( \frac{1}{\sqrt{\pi} l} \right)^{\nu} \begin{cases} e^{-q^2} & \text{if } 0 \leq q \leq 3 \\ 0 & \text{if } q > 3 \end{cases} \quad \text{with} \quad q = \frac{|x - x_0|}{l}$$

- The ***cubic B-spline function***

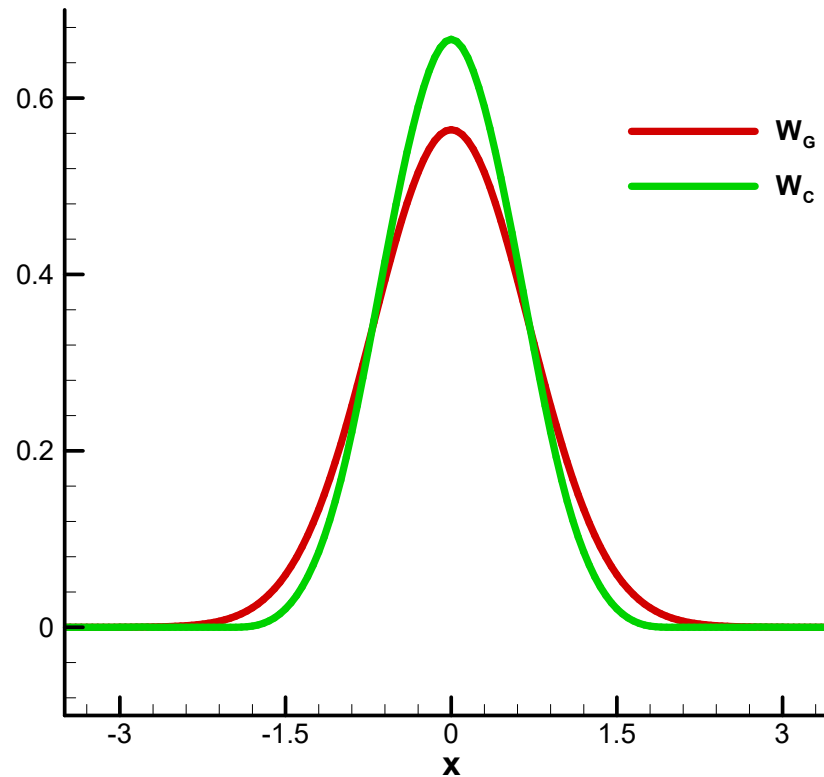
$$W_C(q, l) = \frac{K}{l^\nu} \begin{cases} \frac{2}{3} - q^2 + \frac{1}{2}q^3 & \text{if } 0 \leq q \leq 1 \\ \frac{1}{6}(2 - q)^3 & \text{if } 1 \leq q \leq 2 \\ 0 & \text{if } q > 2 \end{cases}$$

Typically,  $l$  is close to the particle spacing [J.J. Monaghan, 2005].

# Fundamental Aspects

The most widely applied in the SPH simulations are:

- The ***truncated Gaussian distribution***
- The ***cubic B-spline function***



# Numerical Approximation

The integral is approximated by a ***summation form***, over a finite set of  $N$  particles which reconstruct the physical domain  $\Omega$  of the fluid:

$$f(x_i) = \int_{\Omega} f(x') W(x_i - x', l) dx' \quad \Rightarrow \quad f_i = \sum_{j=1}^N V_j f_j W_{ij}$$
$$f_i = \sum_{j=1}^N \frac{m_j}{\rho_j} f_j W_{ij}$$

where  $V_j$  is the volume associated with the  $j^{th}$  particle. Similarly,  $m_j$  and  $\rho_j$  denote the mass and the density.

Although the summation is over all the particles, *only the neighbours* interact with the  $i^{th}$  particle because the smoothing function assigns a ***weight*** to each particle in the *interpolation procedure*, based on the reciprocal positions of the interpolation points.

# Numerical Approximation

The integral is approximated by a ***summation form***, over a finite set of  $N$  particles which reconstruct the physical domain  $\Omega$  of the fluid:

$$\nabla f(x_i) = \int_{\Omega} f(x') \nabla W(x_i - x', l) dx' \quad \Rightarrow \quad \begin{aligned} \nabla f_i &= \sum_{j=1}^N V_j f_j \nabla W_{ij} \\ \nabla f_i &= \sum_{j=1}^N \frac{m_j}{\rho_j} f_j \nabla W_{ij} \end{aligned}$$

To obtain *higher accuracy*:

$$\nabla f_i = \sum_{j=1}^N \frac{m_j}{\rho_j} (f_j - f_i) \nabla W_{ij}$$

and an alternative representation:

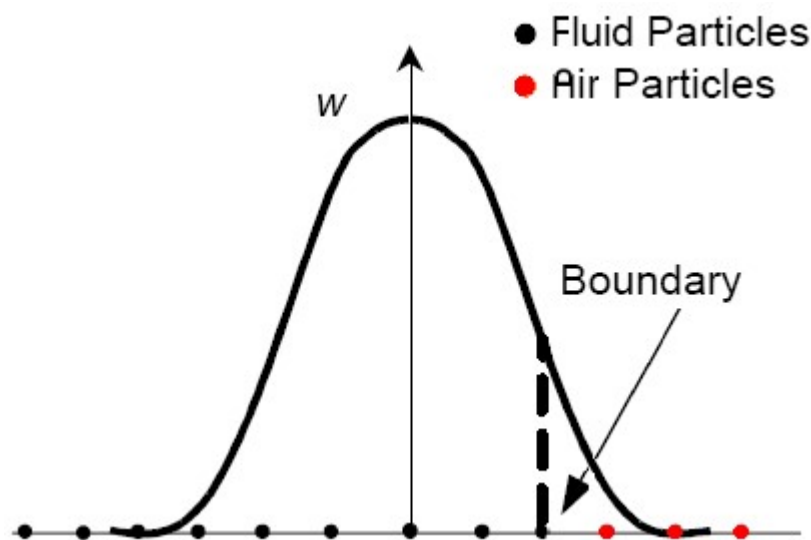
$$\nabla f_i = \rho_i \sum_{j=1}^N m_j \left( \frac{f_j}{\rho_j^2} + \frac{f_i}{\rho_i^2} \right) \nabla W_{ij}$$

## Remarks

The accuracy of the *kernel estimation* depends on the *distribution of the observation points*.

# Boundary Conditions

- 1) The *free surface boundary conditions* are automatically satisfied with the SPH method.



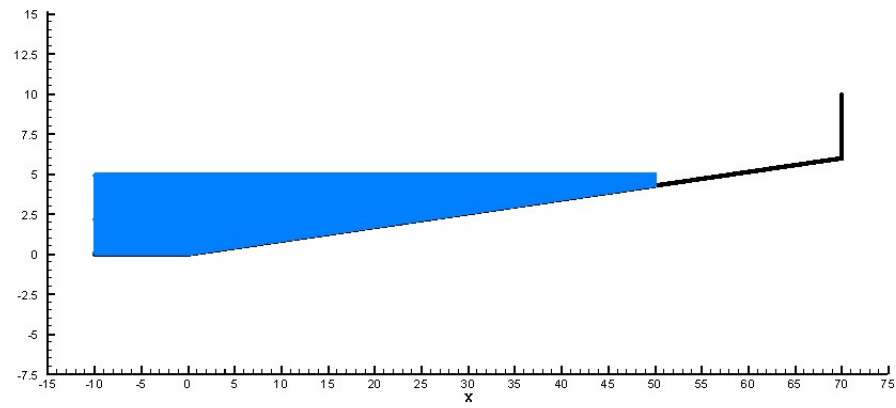
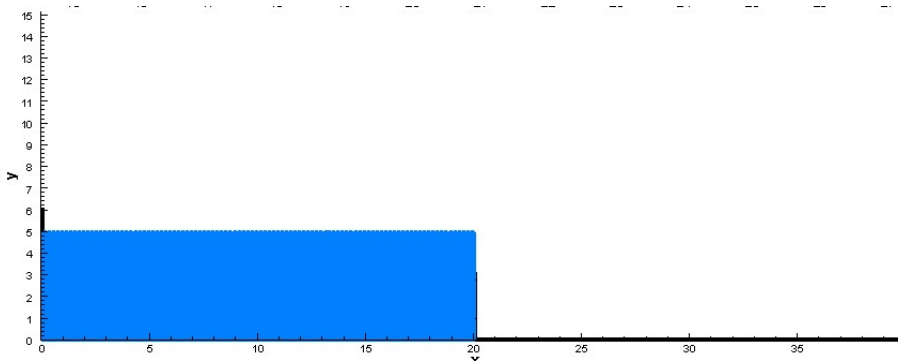
# Boundary Conditions

- 2) The enforcement of the *solid boundary conditions* is to prevent the penetration of fluid particles through the boundaries.

The conditions for fixed or moving solid boundary can be handled using:



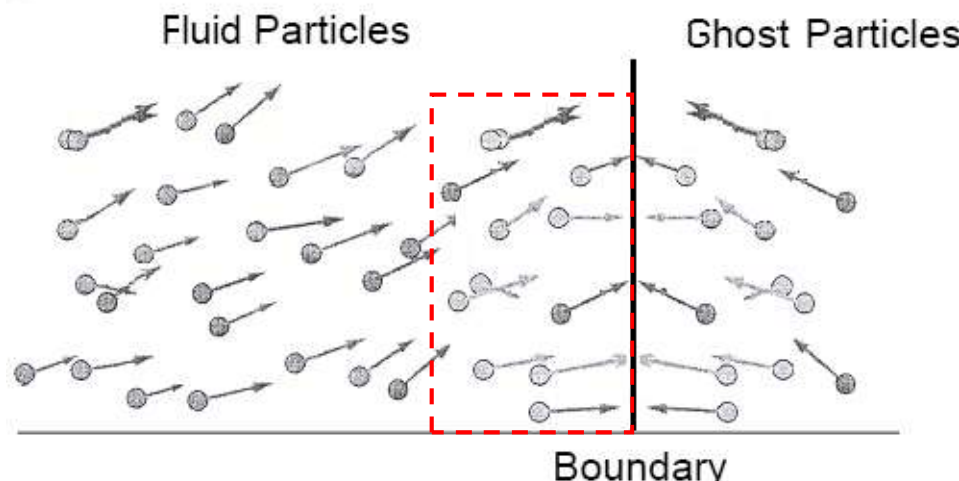
- The “*ghost particles*” technique;
- The *boundary forces* [J.J. Monaghan, 1994].



# Ghost Particles

A solid body is simulated by putting a layer of *ghost particles* along the body.

The solid surface acts as a *mirror* reflecting the real fluid particles, *outside the physical domain*.



[A. Colagrossi, 2004]

The pressure  $p$ , the density  $\rho$  and the velocity  $\mathbf{u}$  are deduced from those of the real fluid particles close to the boundary (within the red box).

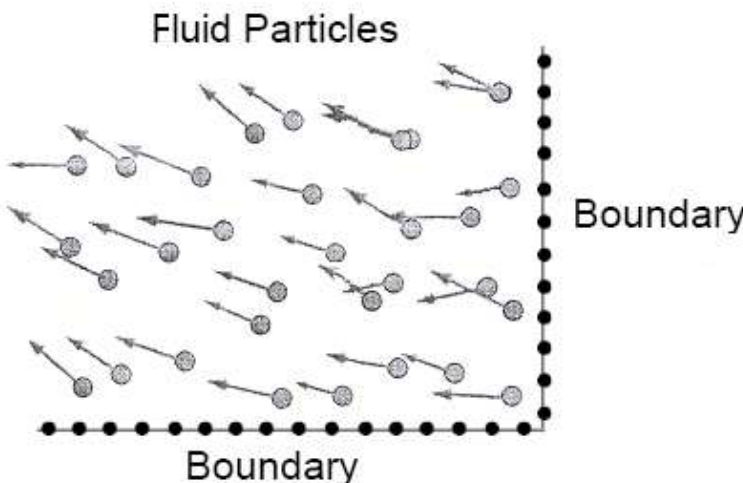
# Boundary Forces

The surfaces of rigid bodies consist of particles which interact with the fluid exerting a *repulsive force*.

It has the form of the Lennard–Jones force and acts as a molecular central force:

$$(F_{ij})^B = \begin{cases} D \left[ \left( \frac{r_0}{|\mathbf{r}_{ij}|} \right)^4 - \left( \frac{r_0}{|\mathbf{r}_{ij}|} \right)^2 \right] \frac{\mathbf{r}_{ij}}{|\mathbf{r}_{ij}|^2} & \text{if } |\mathbf{r}_{ij}| \leq r_0 \\ 0 & \text{if } |\mathbf{r}_{ij}| > r_0 \end{cases}$$

with  $r_0$  is taken to be the initial spacing between the particles and  $D$  is a coefficient.



# Boundary Conditions

<i>Ghost particles</i>	<i>Boundary Forces</i>
They can not easily treat domains with corners or non-convex domains.	They have a larger <i>flexibility</i> and can simulate an arbitrarily moving rigid body with complex shape.
They require more care, in particular for curved surfaces.	They are easy to implement.
<i>No parameters.</i>	They require <i>parameters</i> to calibrate.
They produce a <i>smoother behaviour</i> of the particles near the boundaries and a <i>correct pressure field</i> along the solid.	They cause <i>oscillations</i> in the numerical profiles for the particles close to the boundaries, before to find the <i>equilibrium position</i> .
Do not reduce considerably the <i>time step</i> .	They can reduce considerably the <i>time step</i> , or they need <b>implicit time integration</b>

## The Original SPH Formulation of Gingold & Monaghan

The SPH scheme applied to the equations of ***hydrodynamics for an ideal weakly compressible fluid***:

$$\begin{cases} \frac{d\rho}{dt} = -\rho \nabla \cdot \mathbf{u} \\ \frac{d\mathbf{u}}{dt} = -\frac{1}{\rho} \nabla p + \mathbf{g} \\ \frac{d\mathbf{x}}{dt} = \mathbf{u} \end{cases} \quad \Rightarrow \quad \begin{cases} \rho_i^{n+1} = \rho_i^n - \Delta t \sum_{j=1}^N m_j ((\mathbf{u}_j^n - \mathbf{u}_i^n) \cdot \nabla W_{ij}) \\ \mathbf{u}_i^{n+1} = \mathbf{u}_i^n - \Delta t \sum_{j=1}^N m_j \left( \frac{p_j^n}{(\rho_j^n)^2} + \frac{p_i^n}{(\rho_i^n)^2} + \Pi_{ij} \right) \nabla W_{ij} + \mathbf{g} \\ \mathbf{x}_i^{n+1} = \mathbf{x}_i^n + \mathbf{u}_i^{n+1} \Delta t \end{cases}$$

The equation of state:

$$p = k_0 \left( \left( \frac{\rho}{\rho_0} \right)^\gamma - 1 \right) \quad c^2 = \frac{\gamma k_0}{\rho_0} \left( \frac{\rho}{\rho_0} \right)^{\gamma-1}$$

The method needs an **artificial diffusion** term to be stabilized  
(SPH kernel summation is a central finite difference, which is  
unconditionally unstable with first order Euler time integration)

# Vila formulation

The SPH equations of fluid dynamics following Vila:

$$\left\{ \begin{array}{l} \frac{d(\omega_i \Phi_i)}{dt} = -\omega_i \sum_{j=1}^N \omega_j 2\mathbf{G}_{ij} \nabla_i W_{ij} + \omega_i \mathbf{S}_i \\ \frac{d\omega_i}{dt} = \omega_i (\nabla_i \cdot \mathbf{v}_i) \\ \frac{d\mathbf{x}_i}{dt} = \mathbf{v}_i \\ \Phi_i = (\rho, \rho\mathbf{v})_i \end{array} \right.$$

ICs:  $\begin{cases} \Phi_i(0) = \Phi^0(\mathbf{x}_i) \\ \omega_i(0) = \omega_i^0 \\ \mathbf{x}_i(0) = \mathbf{x}_i^0 \end{cases}$

EOS:  $p = k_0 \left( \left( \frac{\rho}{\rho_0} \right)^\gamma - 1 \right)$

where  $\omega_i$  is a weight, that can be physically interpreted as particle volume and that also takes into account deformations due to the velocity field  $\mathbf{v}$ .  $\mathbf{G}$  is the flux evaluated by a Riemann solver, such as e.g. the exact Godunov flux:

$$\mathbf{G}_{ij} = \mathbf{F}(\Phi^E) \mathbf{n}_{ij} \quad \Phi^E = \Phi^E(\Phi_i, \Phi_j) \quad \text{Solution of the Riemann-Problem between particles } i \text{ and } j$$

Note that the artificial viscosity  $\Pi$  is replaced by an intrinsic numerical viscosity that needs *no parameters* to be fixed and *improves the stability*.

# A New SPH Formulation

The SPH scheme applied to the equations of ***hydrodynamics for an ideal weakly compressible fluid***:

$$\begin{cases} \frac{d\rho}{dt} = -\rho \nabla \cdot \mathbf{u} \\ \frac{d\mathbf{u}}{dt} = -\frac{1}{\rho} \nabla p + \mathbf{g} \\ \frac{d\mathbf{x}}{dt} = \mathbf{u} \end{cases} \quad \Rightarrow \quad \begin{cases} \rho_i^{n+1} = \rho_i^n - \Delta t \sum_{j=1}^N m_j (\Delta \mathbf{u}_{ij}^n \cdot \nabla W_{ij} - \mathbf{n}_{ij} \cdot \nabla W_{ij} (c_{ij}^{\max} / \rho_j^n (\rho_j^n - \rho_i^n))) \\ \mathbf{u}_i^{n+1} = \mathbf{u}_i^n - \Delta t \sum_{j=1}^N m_j \left( \frac{p_j^n}{(\rho_j^n)^2} + \frac{p_i^n}{(\rho_i^n)^2} \right) \nabla W_{ij} + \mathbf{g} \\ \mathbf{x}_i^{n+1} = \mathbf{x}_i^n + \mathbf{u}_i^{n+1} \Delta t \end{cases}$$

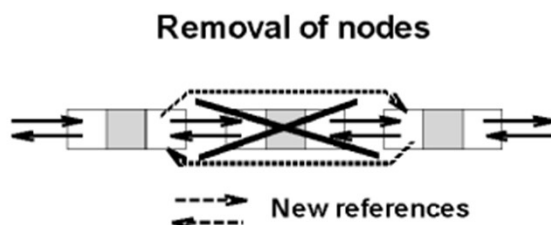
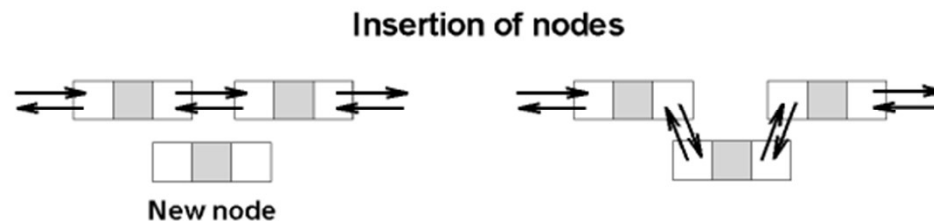
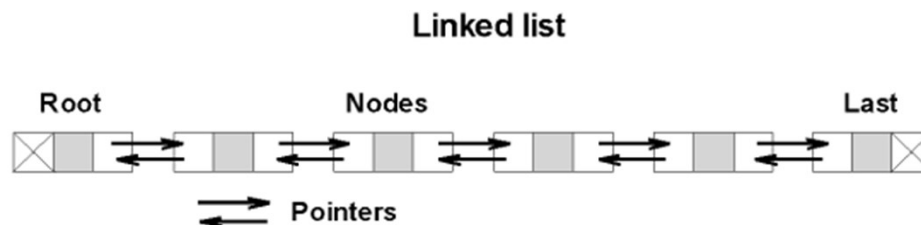
The equation of state:  $p = k_0 \left( \left( \frac{\rho}{\rho_0} \right)^\gamma - 1 \right)$        $\Delta \mathbf{u}_{ij}^n = \mathbf{u}_j^n - \mathbf{u}_i^n$

The ***new SPH formulation*** is able to provide good solution for the particle positions preserving the numerical accuracy for the pressure field.

# Some Comments on Implementation

Management of the data in a very flexible way using  
**LINKED LISTS** and **POINTERS**.

- *The particles can be deleted or added, following the motion of the fluid.*



# Convergence Test

The convergence test has been carried out on the numerical solutions of the dam break problem in 3D at time:     $t = 1.2\text{s}$                $t = 1.5\text{s}$                $t = 2.0\text{s}$

⇒ ***250'000 particles***

Videoclip [CG3D\\_0250.avi](#)

using ***32 CPUs***

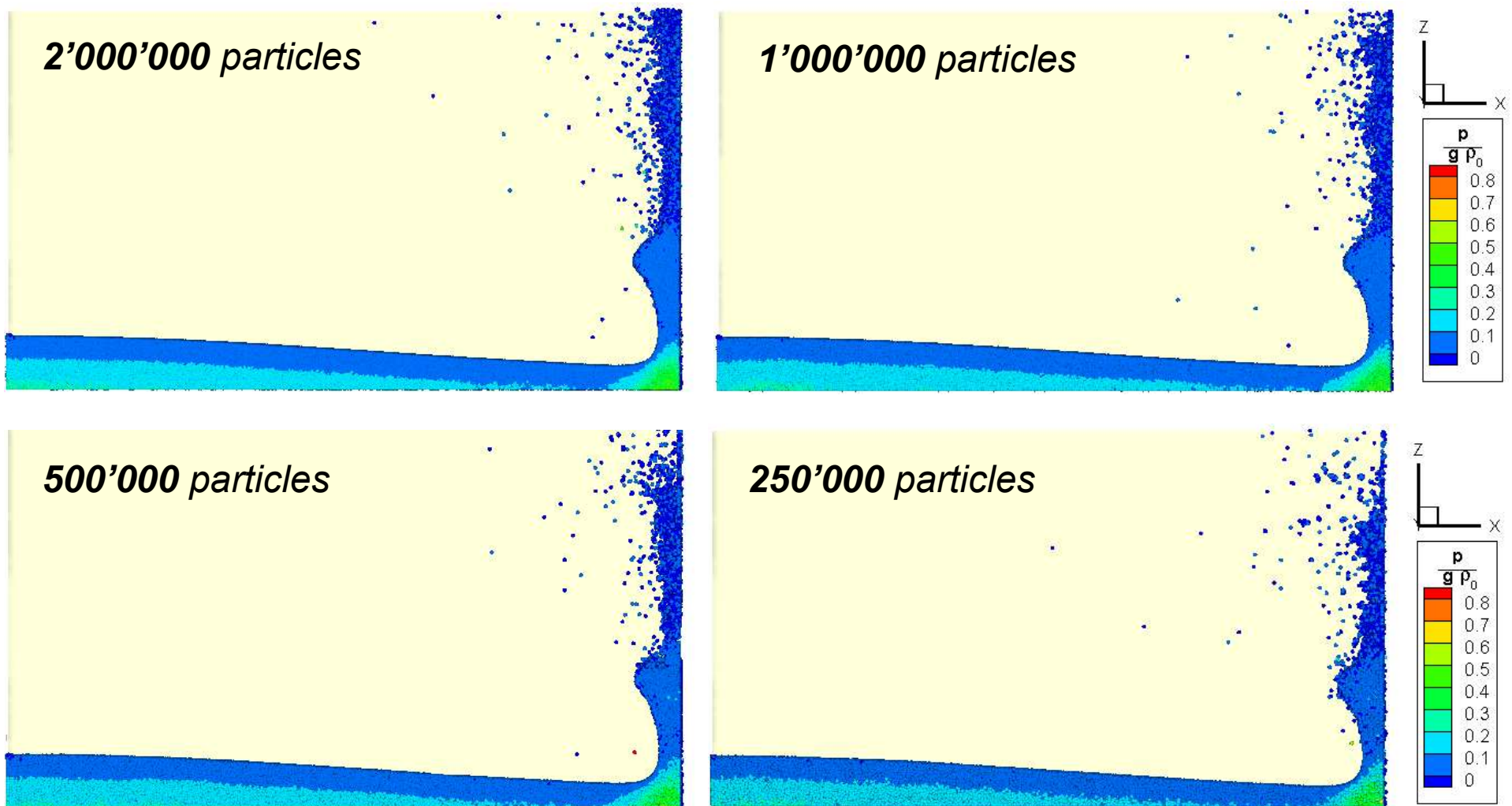
⇒ ***500'000 particles using 64 CPUs***

⇒ ***1'000'000 particles using 128 CPUs***

⇒ ***2'000'000 particles using 256 CPUs***

# Convergence Test

Comparison of the solutions at time  $t = 1.2$  s

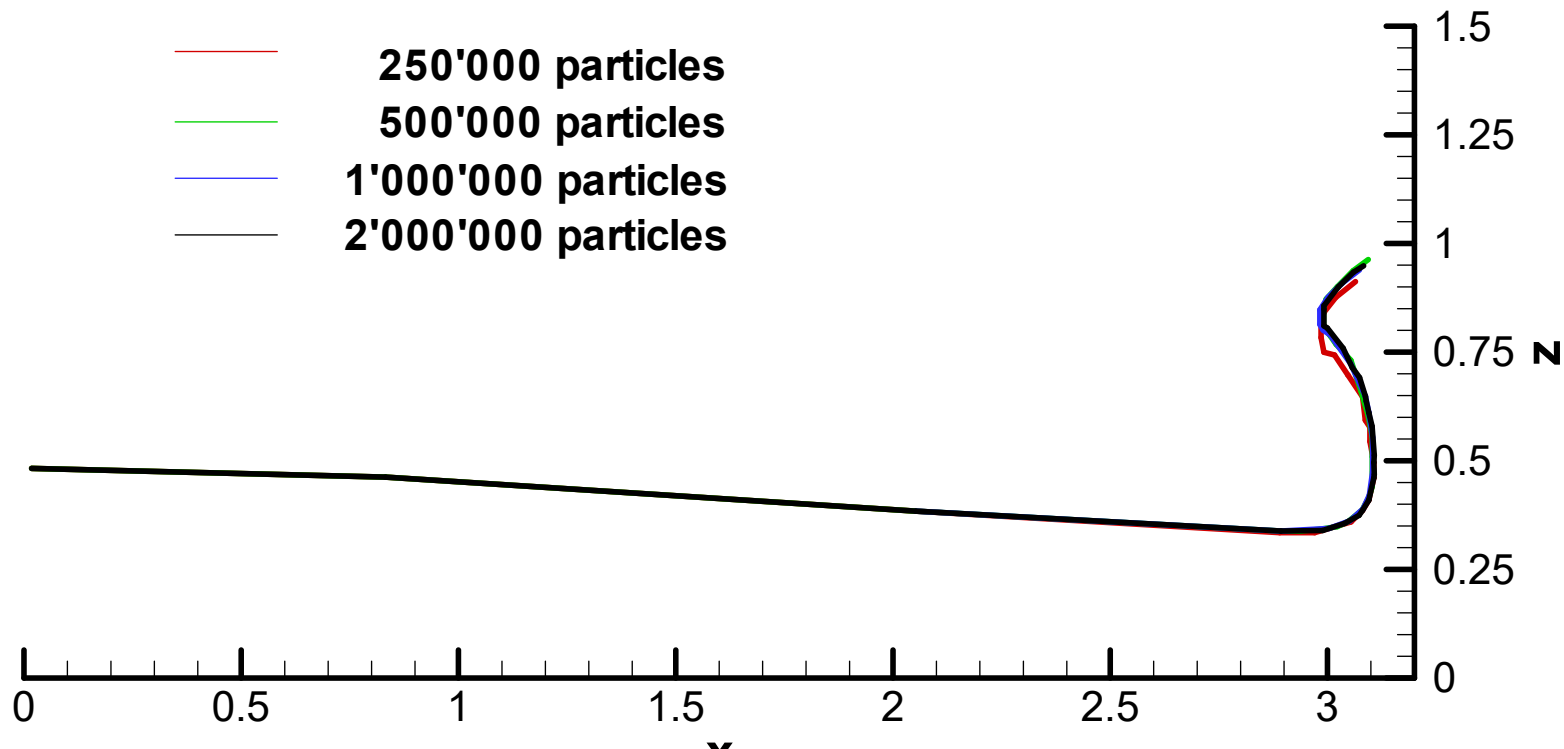


# Convergence Test

The convergence test has been carried out on the dam break problem in 3D.

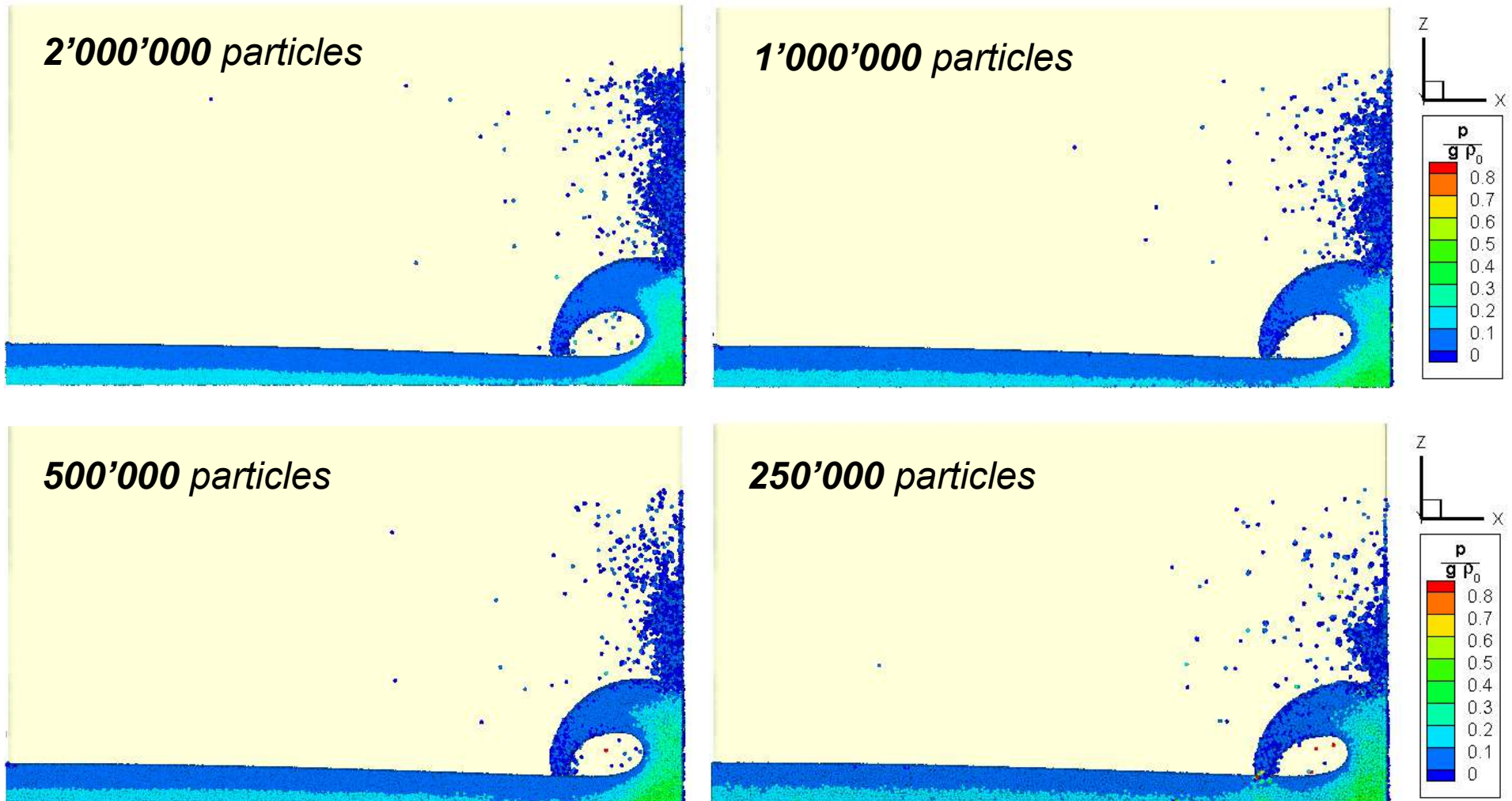
## Comparison of the solutions

at time  $t = 1.2$  s



# Convergence Test

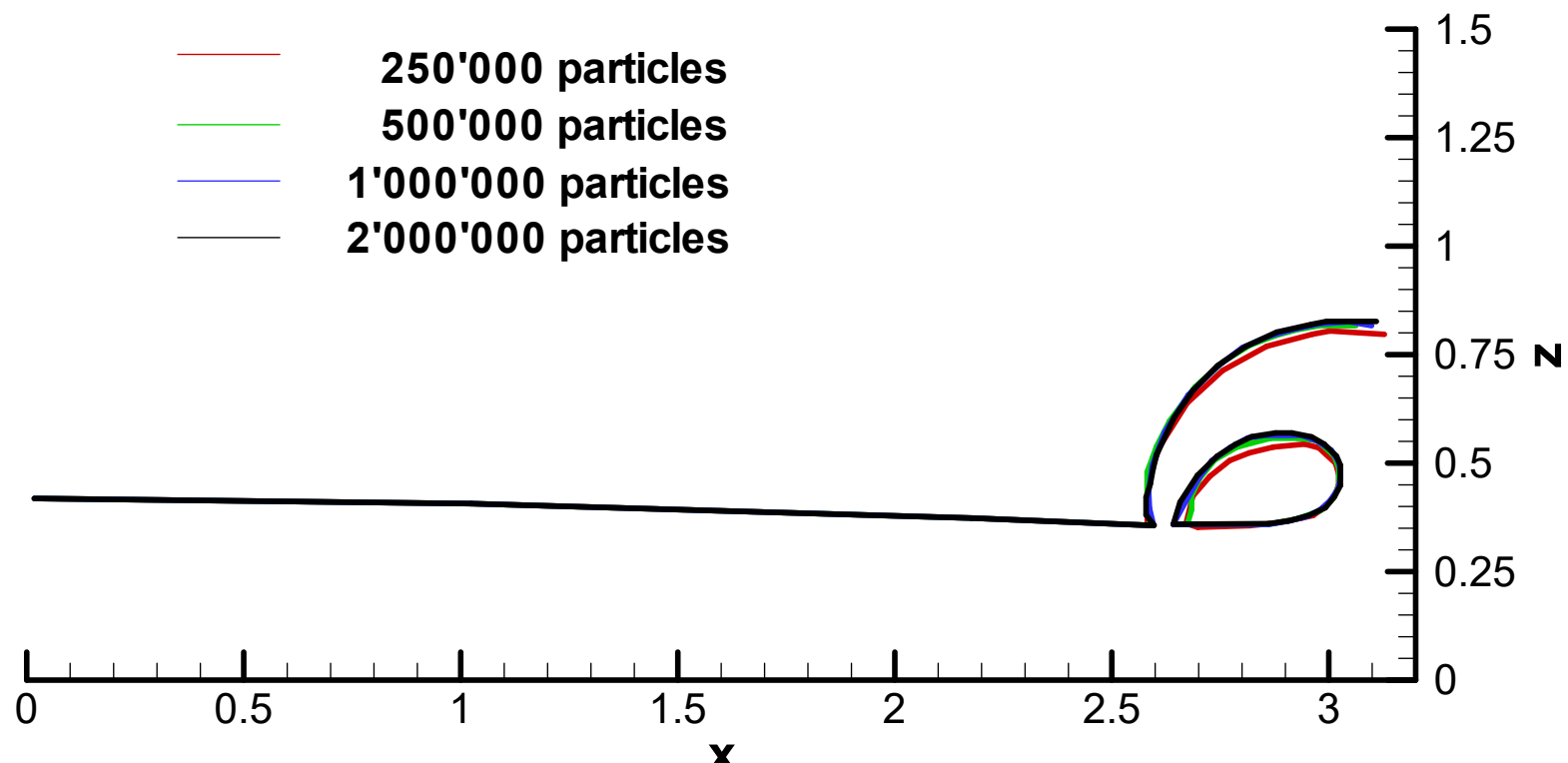
Comparison of the solutions at time  $t = 1.5$  s



# Convergence Test

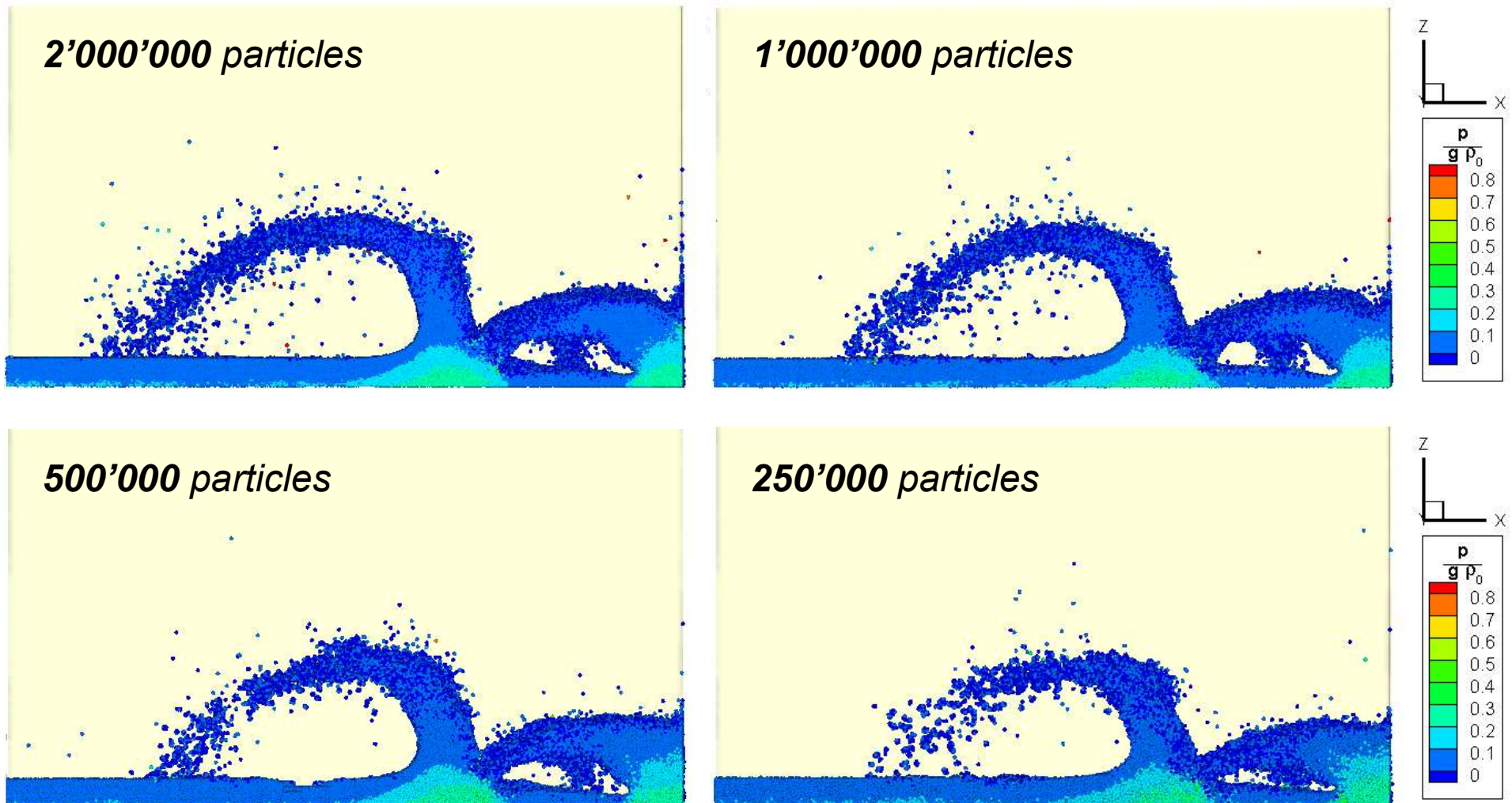
The convergence test has been carried out on the dam break problem in 3D.

**Comparison of the solutions  
at time  $t = 1.5$  s**



# Convergence Test

Comparison of the solutions at time  $t = 2.$  s

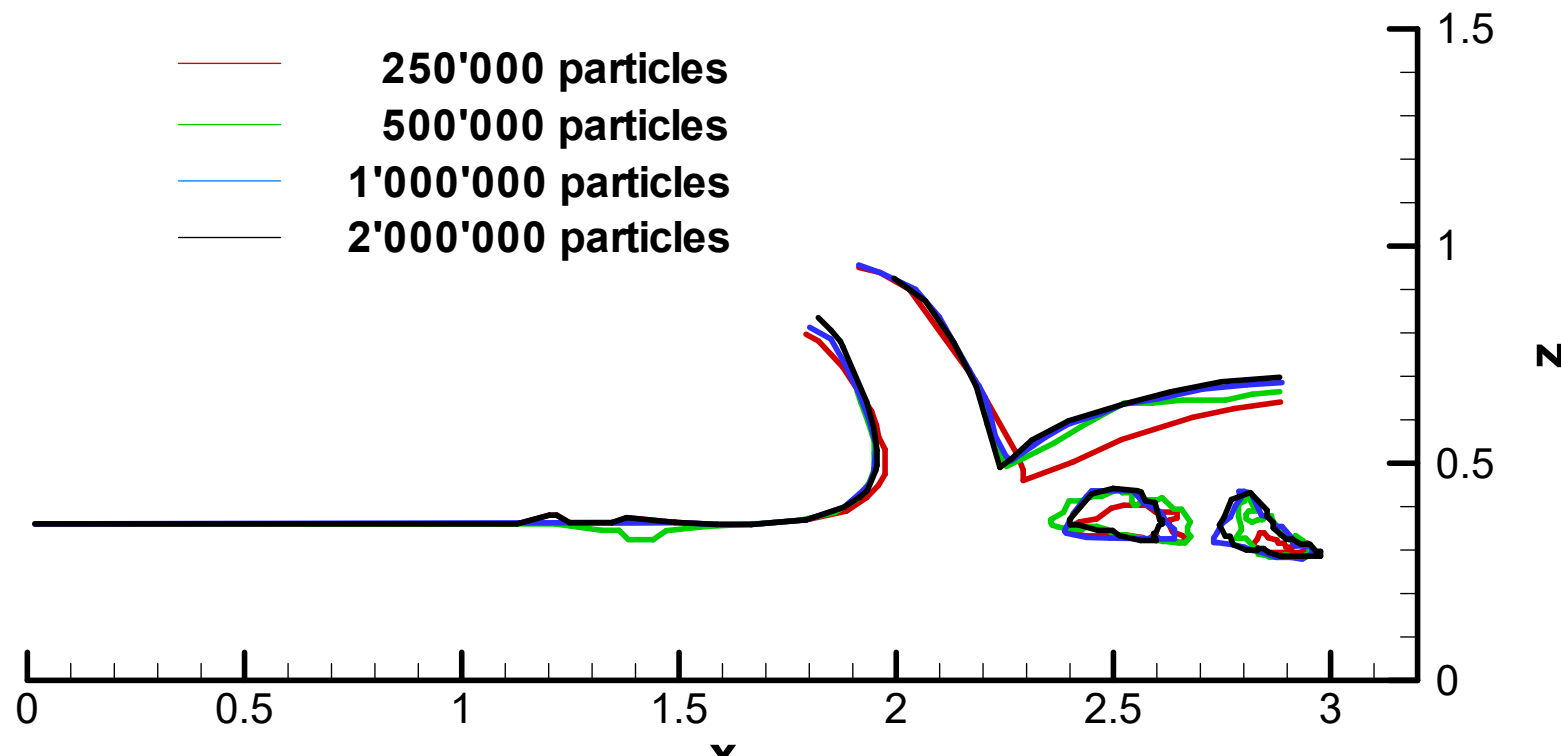


# Convergence Test

The convergence test has been carried out on the dam break problem in 3D.

## Comparison of the solutions

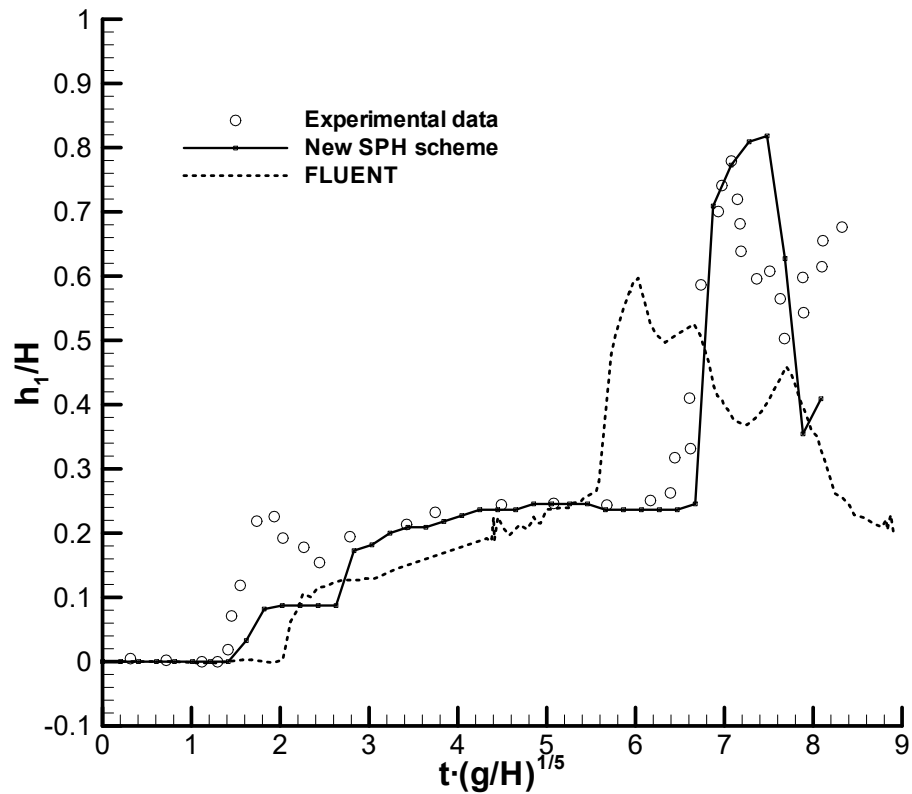
at time  $t = 2.0$  s



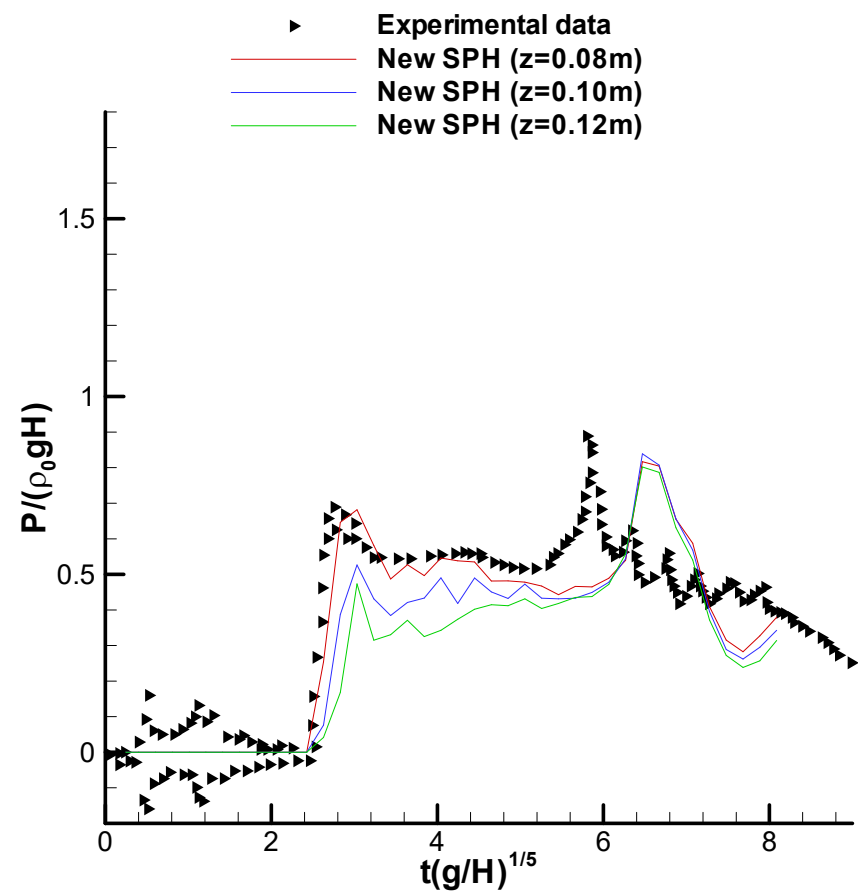
# Comparison with Experimental Data

The numerical solution is compared with the experimental data.

*Water depth*



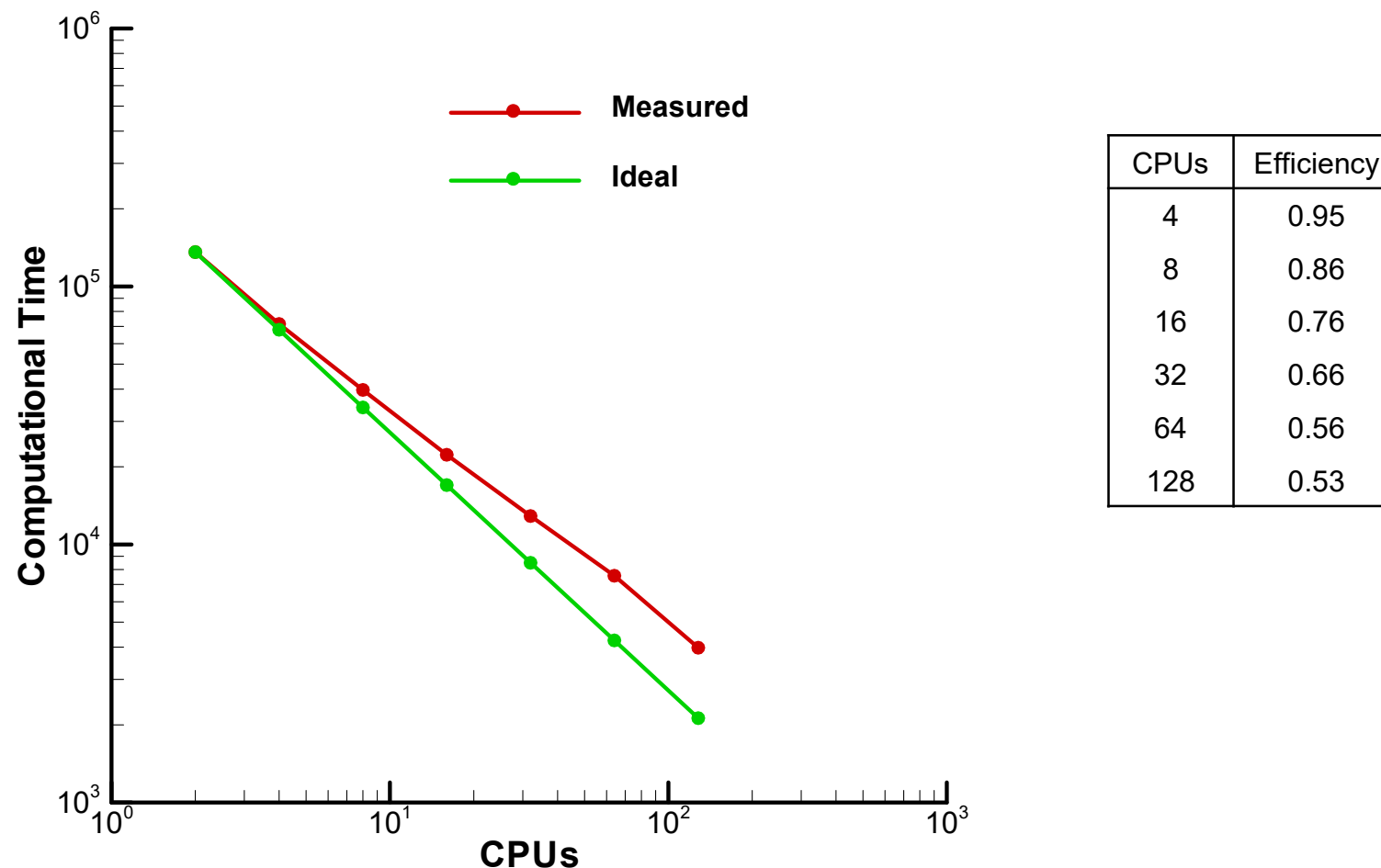
*Pressure field*



Zhou, Z. Q., Kat, J. O. D. and Buchner, B. (1999) 7th Intl. Conf. Num. Ship Hydrodynamics.

# Speed-up

To assess the performance and the efficiency of the numerical implementation, the *speed-up test* has been carried out.

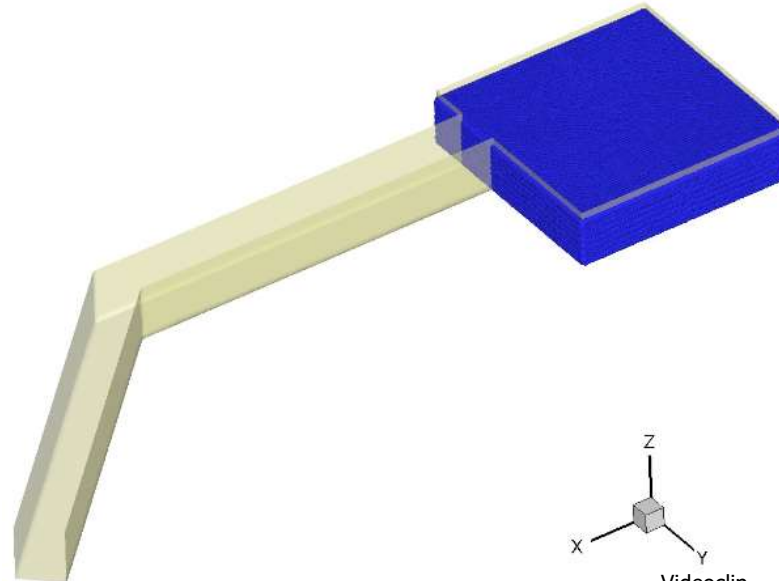


# Applications in 3D

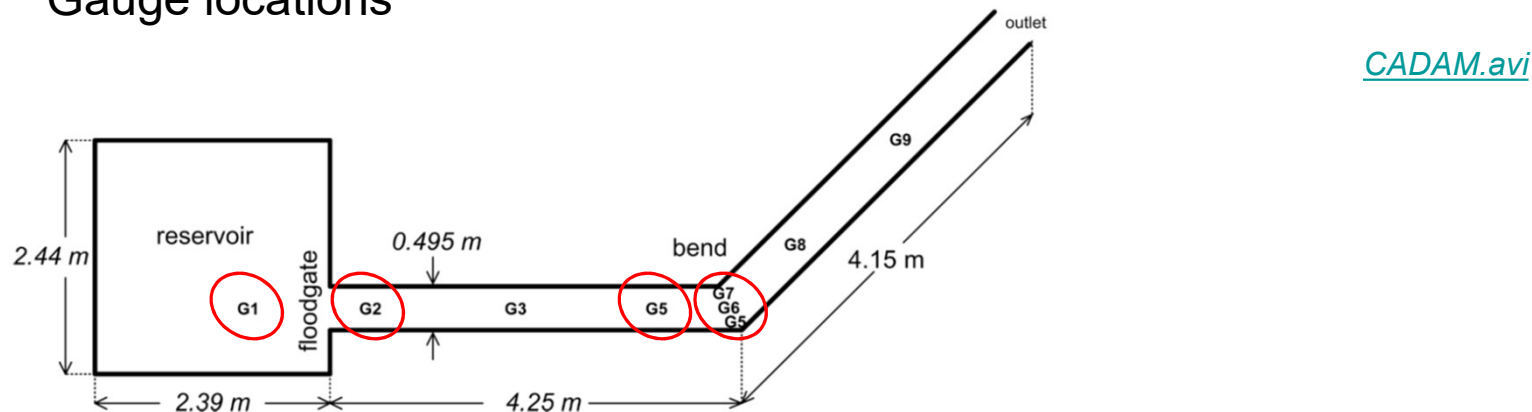
The test case consists of a dam break problem flow in a channel with a 45 degrees bend.

**1'300'000 particles**

**128 CPUs**

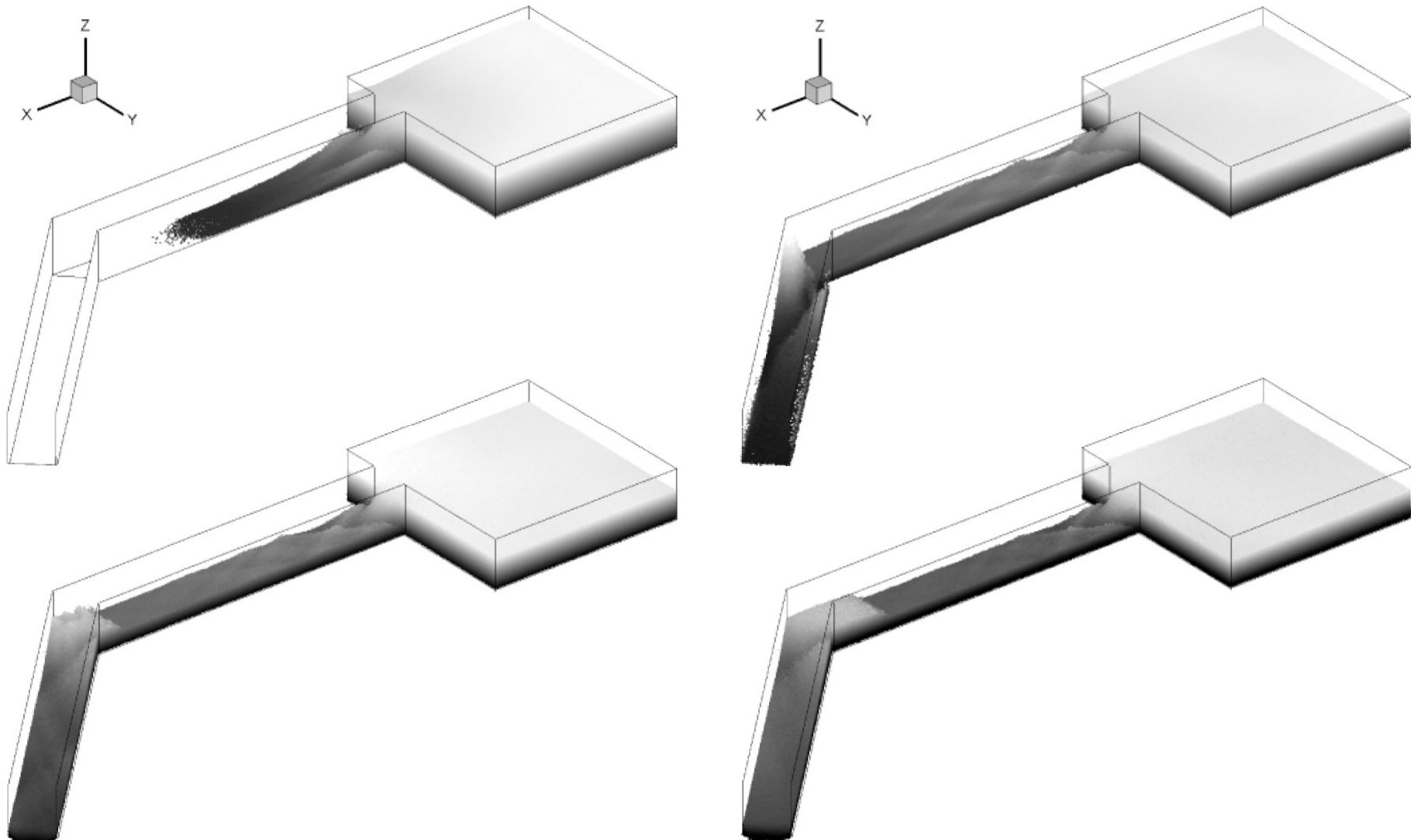


Gauge locations



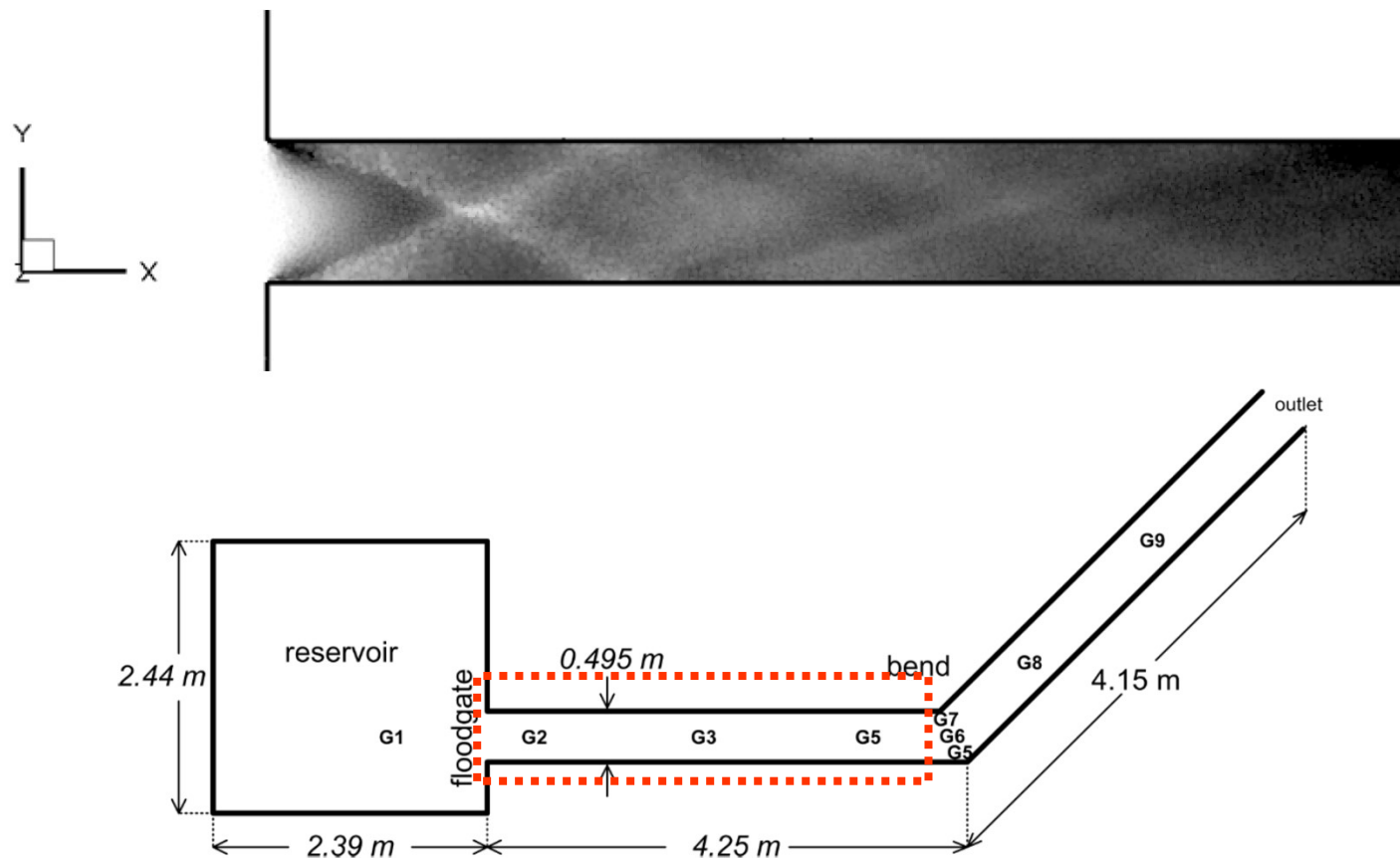
# Applications in 3D

Numerical solutions at time 1s, 4s, 7s, 10s.



# Applications in 3D

Oblique fronts at time 4s on the free surface in the channel upstream the bend.

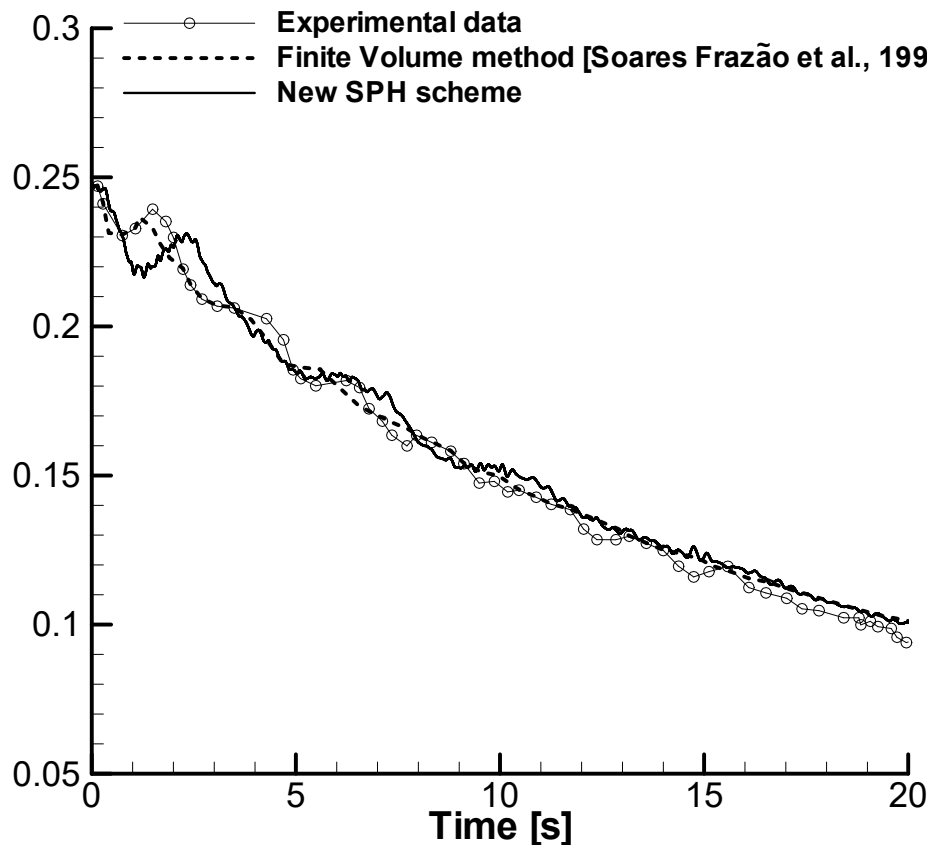


# Applications in 3D

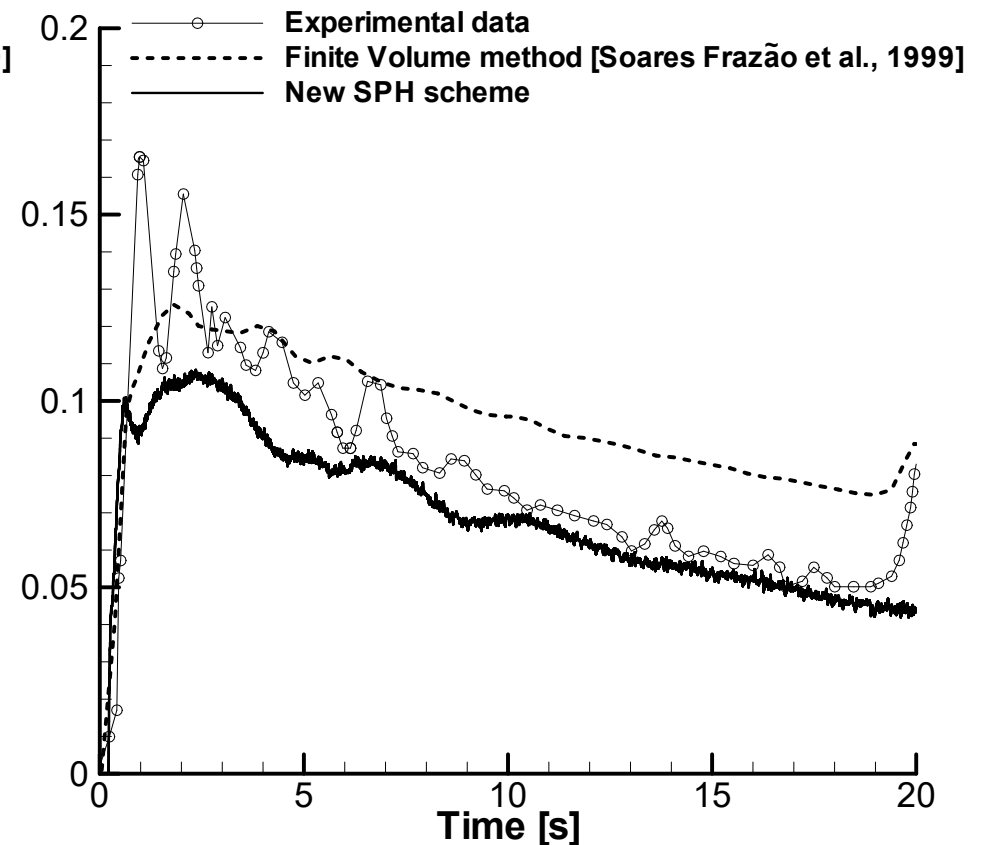
The test case consists of a dam break problem flow in a channel with a 45 degrees bend.

*Water depth as a function of time at gauges.*

G1



G2

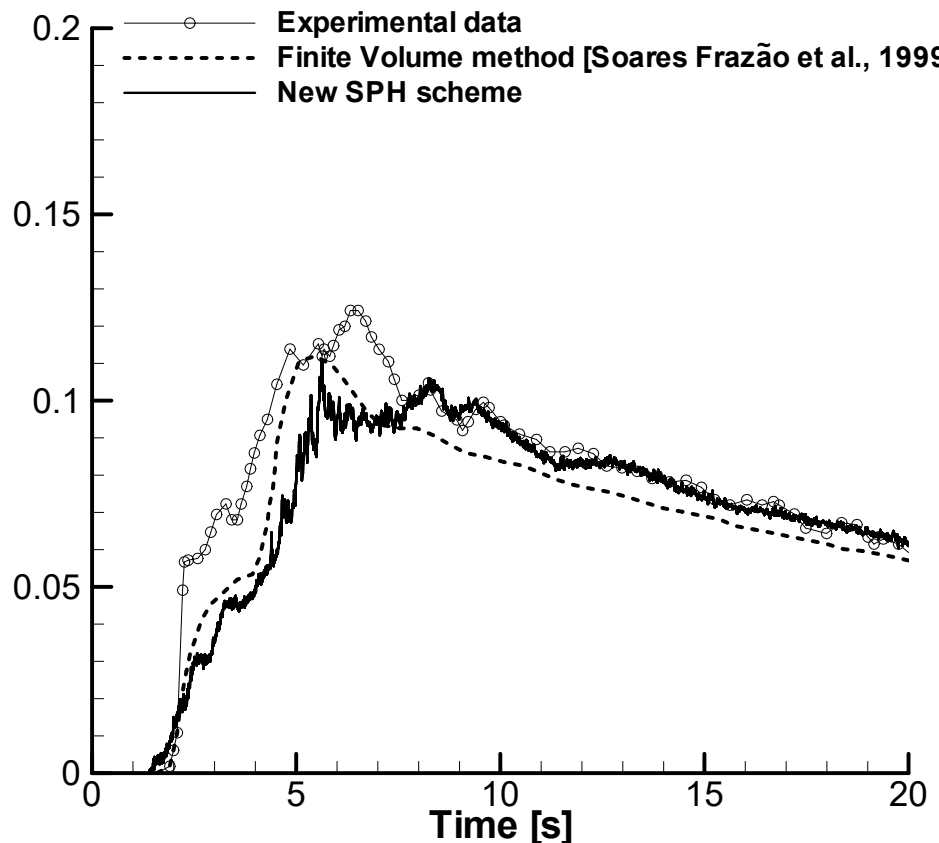


# Applications in 3D

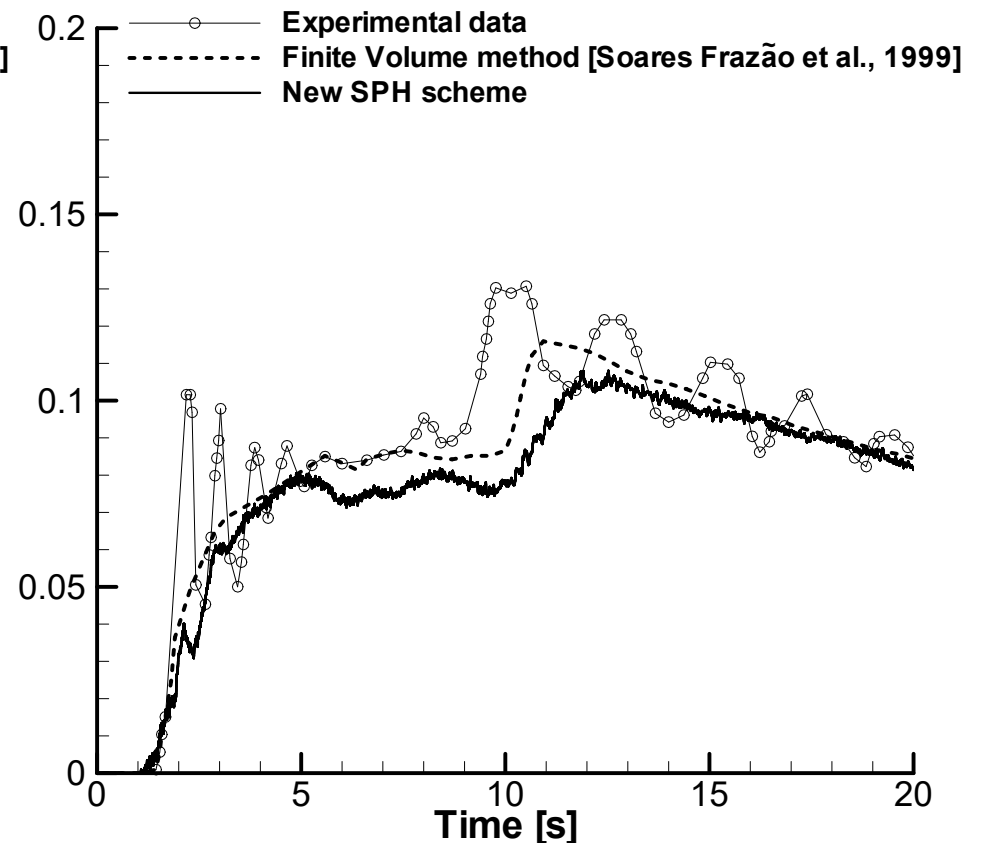
The test case consists of a dam break problem flow in a channel with a 45 degrees bend.

*Water depth as a function of time at gauges.*

**G7**

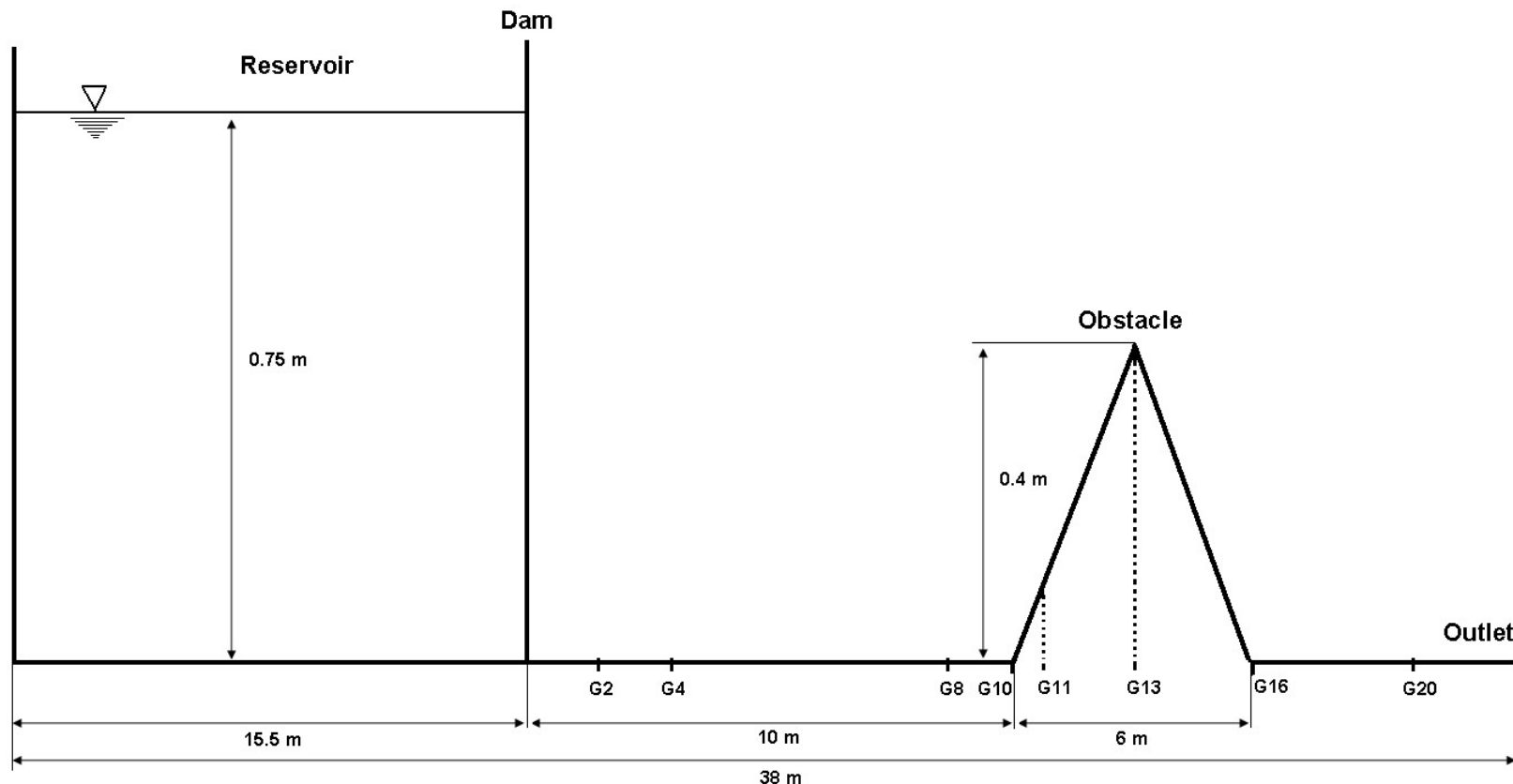


**G4**



# Applications in 3D

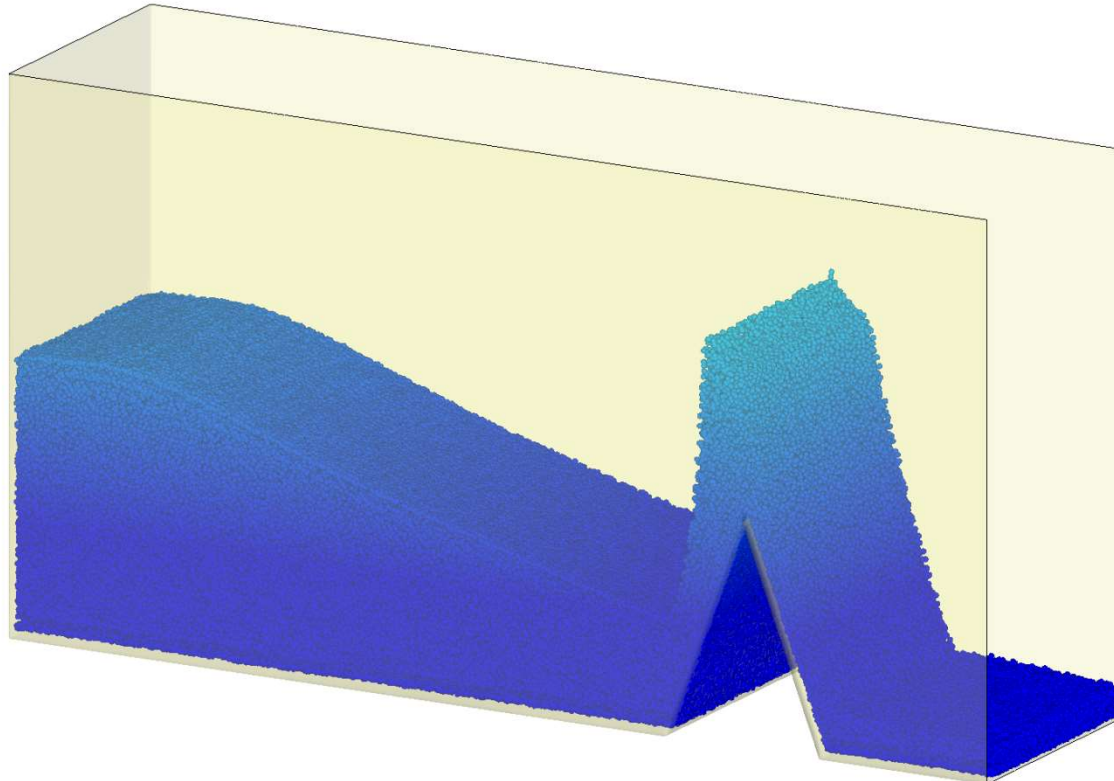
The test case consists of a dam break problem to study the *impact flow* against an *obstacle*, computed in a fully 3D setting.



# Applications in 3D

The test case consists of a dam break problem to study the *impact flow* against an *obstacle*, computed in a fully 3D setting.

**Numerical solution at time  $t = 8.5$  s**

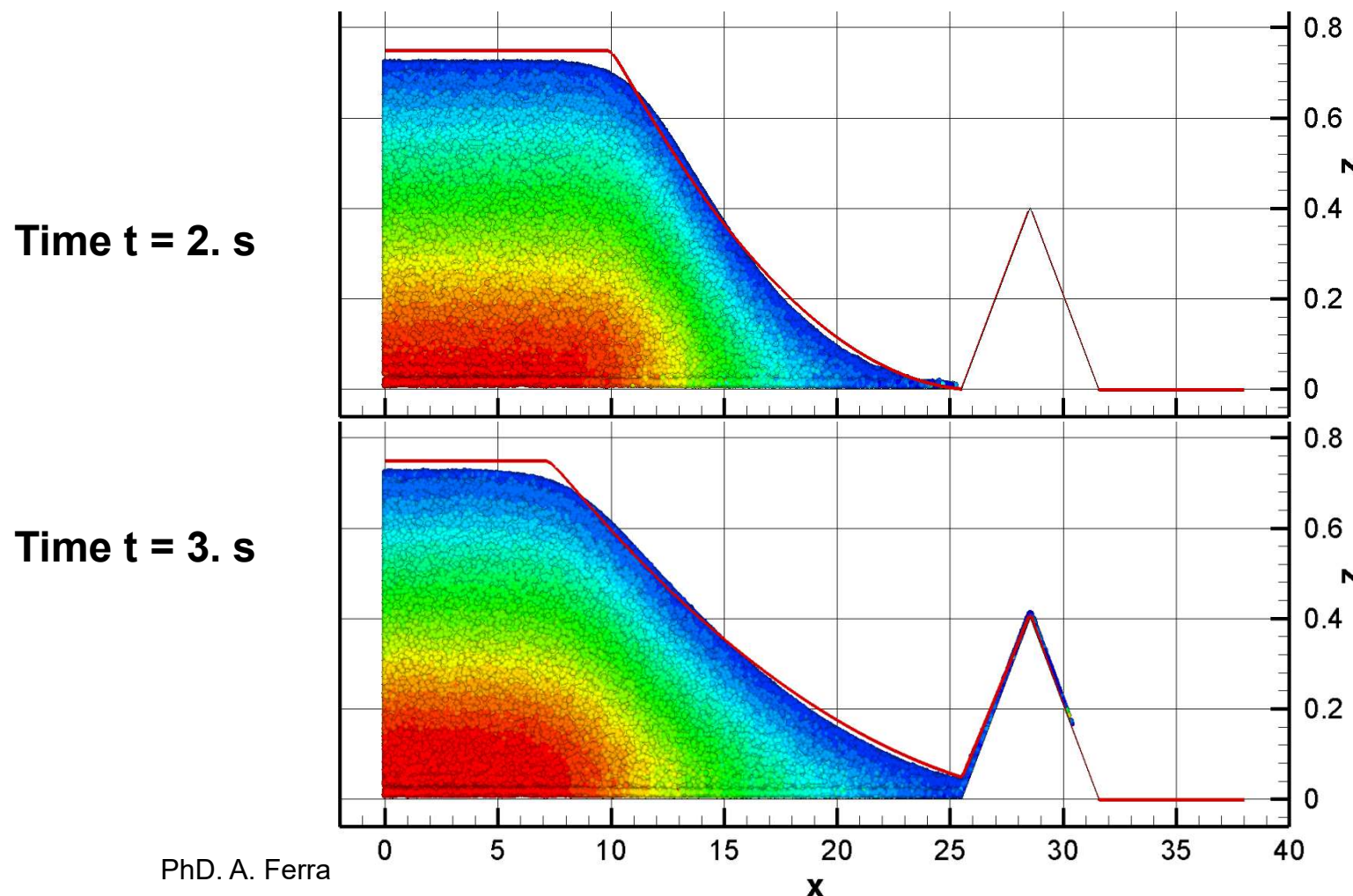


**1'500'000 particles**

**100 CPUs**

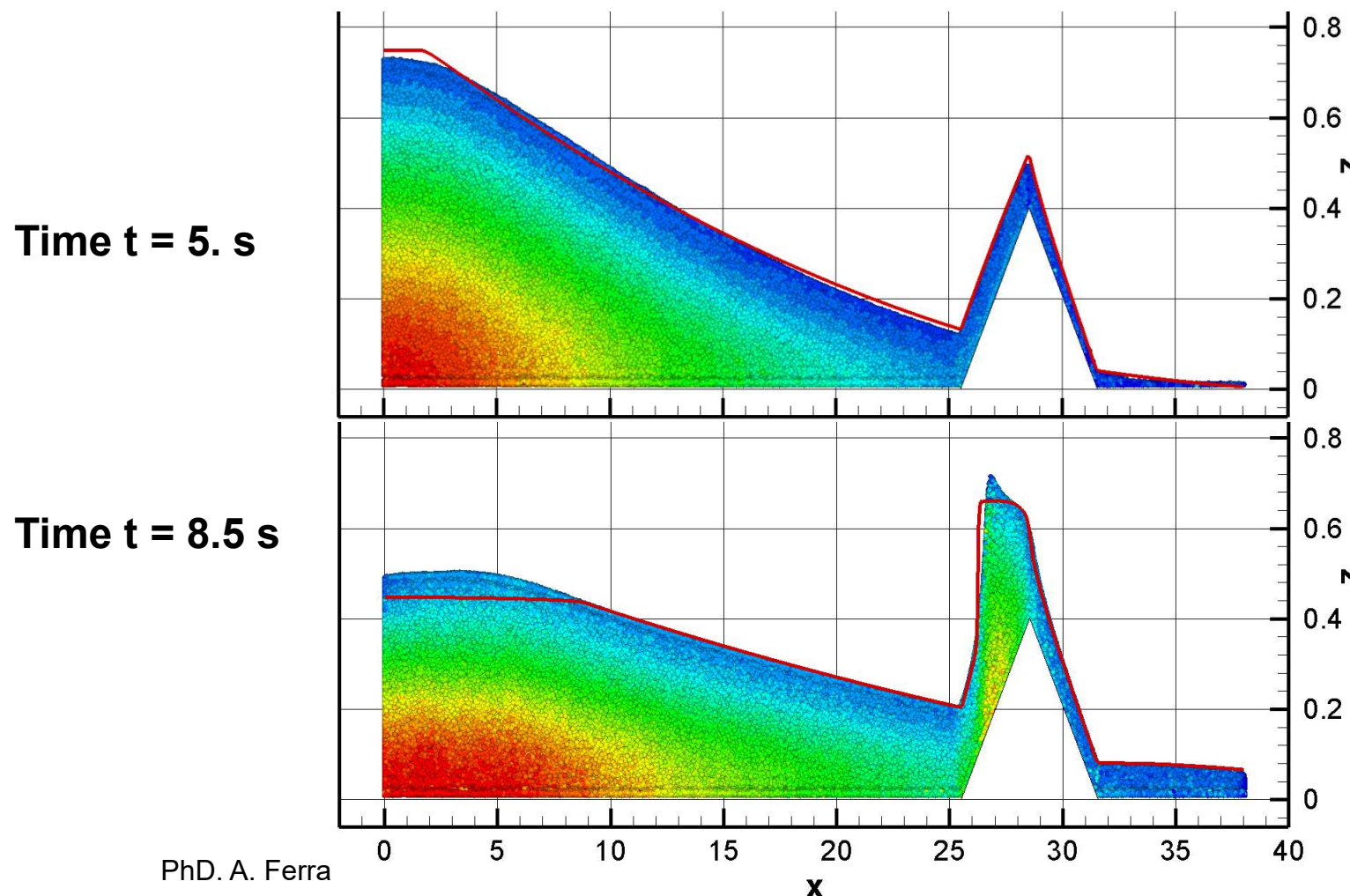
# Applications in 3D

The numerical solution of the 3D parallel SPH compared with the solution of the **1D Finite Volume scheme of third order in space and in time of SWE** with **500 elements** [M. Dumbser].



# Applications in 3D

The numerical solution of the 3D parallel SPH compared with the solution of the **1D Finite Volume scheme of third order in space and in time of SWE** with **500 elements** [M. Dumbser].



# Applications

The test case consists of a *dam break problem down a sloping channel*.

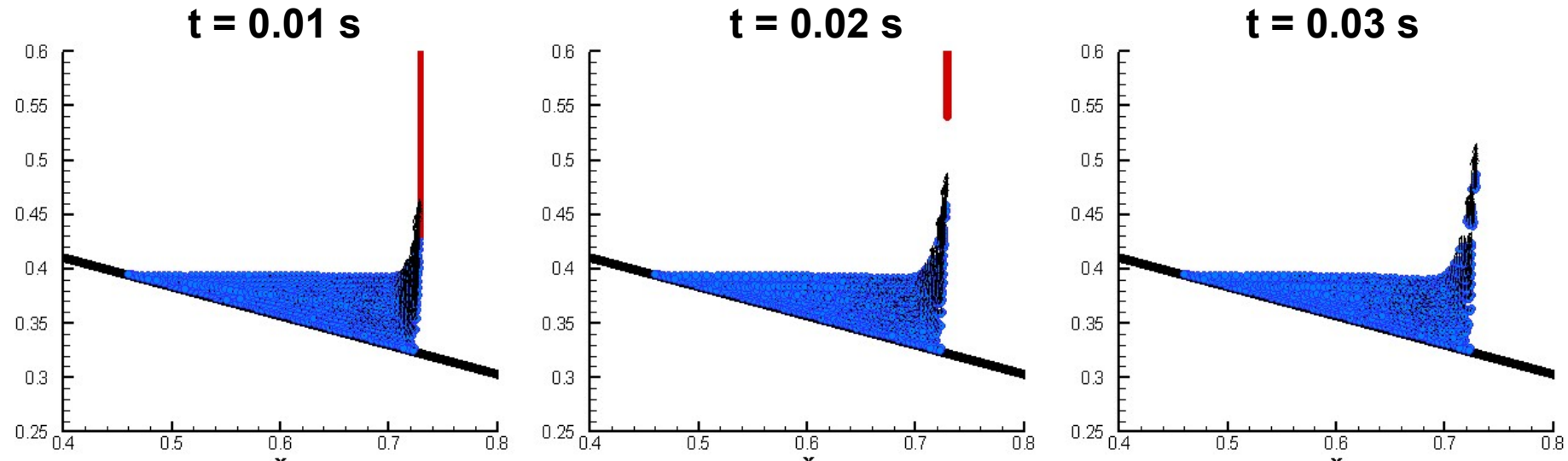
**Newtonian fluid:**

The velocity of the gate is fixed to  $\mathbf{u} = \begin{pmatrix} 0. \\ 3.63 \end{pmatrix} \frac{\text{m}}{\text{s}}$ .

The ***no-slip condition*** of the flow at the wall produces ***adherence phenomena***.



$$\mu_N = 10 \text{ Pa} \cdot \text{s}$$



# Applications

The test case consists of a *dam break problem down a sloping channel*.

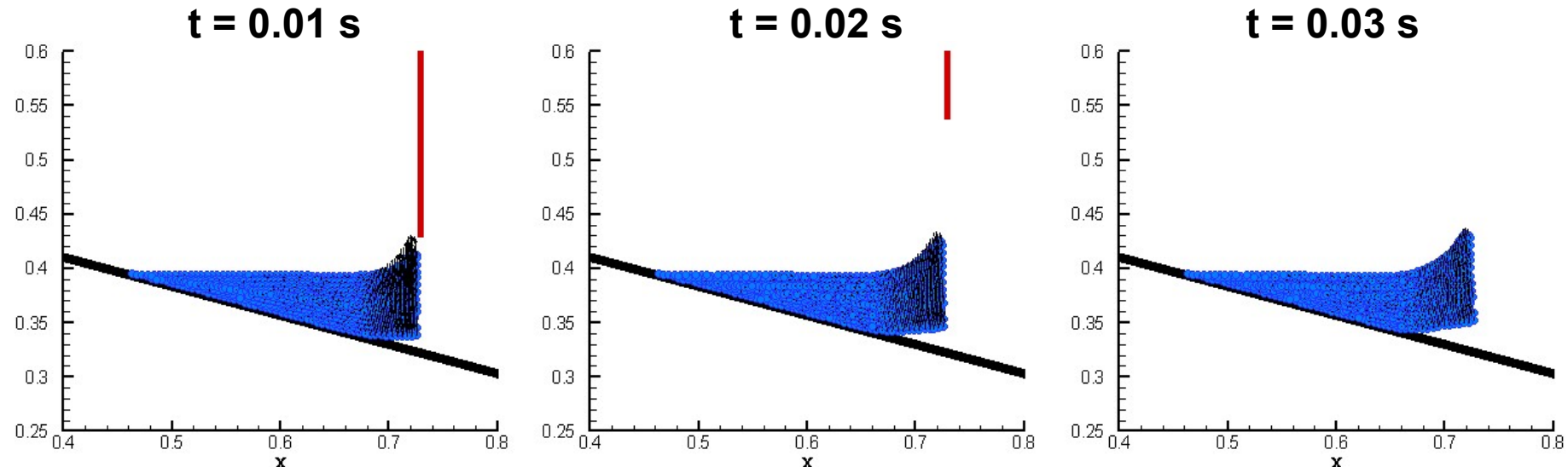
**Newtonian fluid:**

The velocity of the gate is fixed to  $\mathbf{u} = \begin{pmatrix} 0. \\ 3.63 \end{pmatrix} \frac{\text{m}}{\text{s}}$ .

The ***no-slip condition*** of the flow at the wall produces ***adherence phenomena***.



$$\mu_N = 50 \text{ Pa} \cdot \text{s}$$



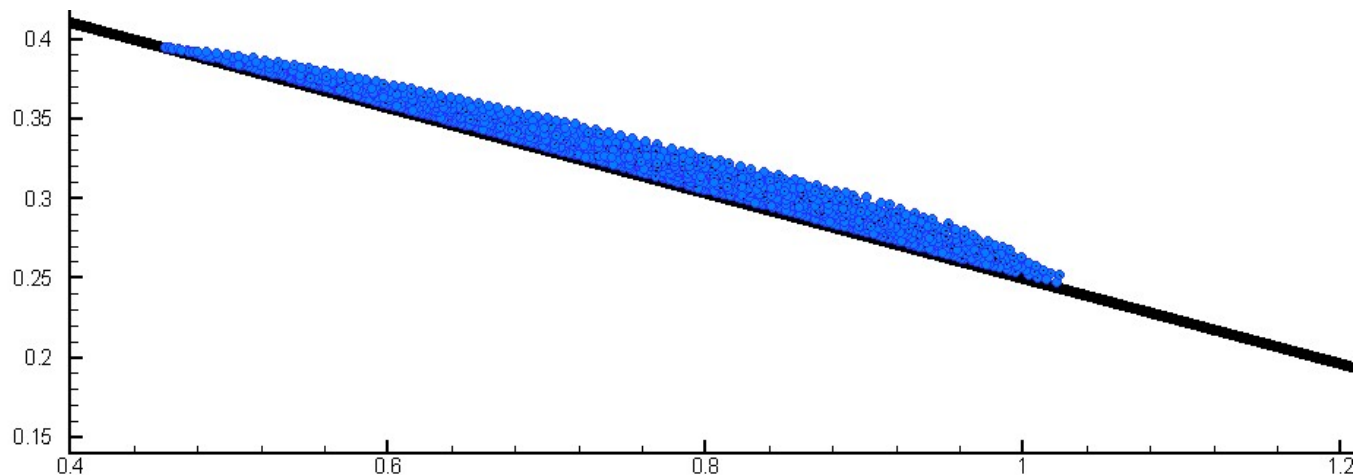
# Applications

The test case consists of a *dam break problem down a sloping channel*.

**Newtonian fluid:**

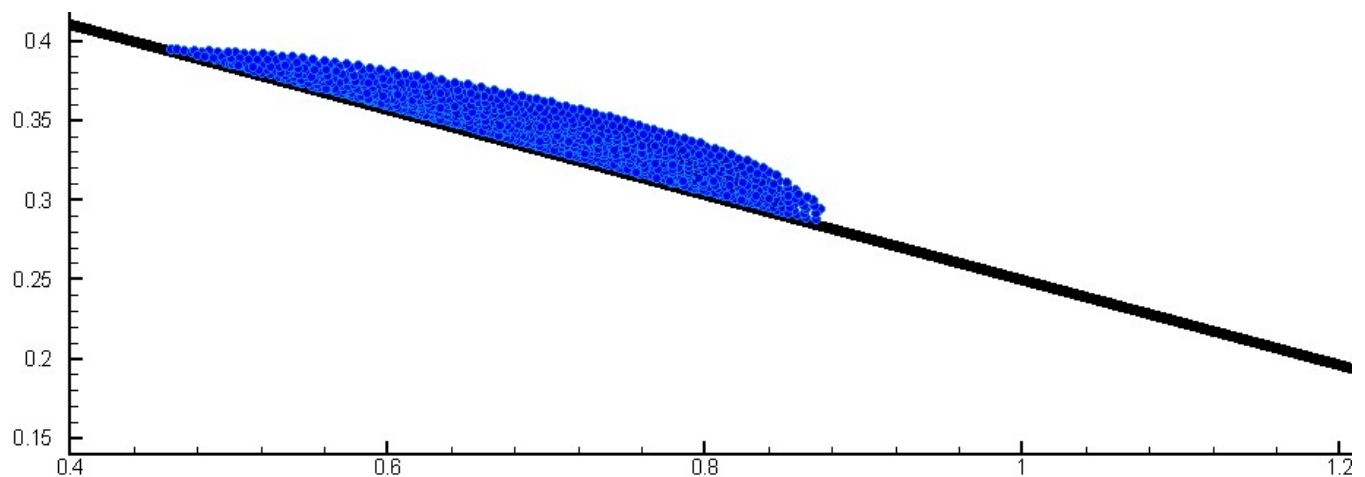
**Time t = 3.5 s**

$$\mu_N = 10 \text{ Pa} \cdot \text{s}$$



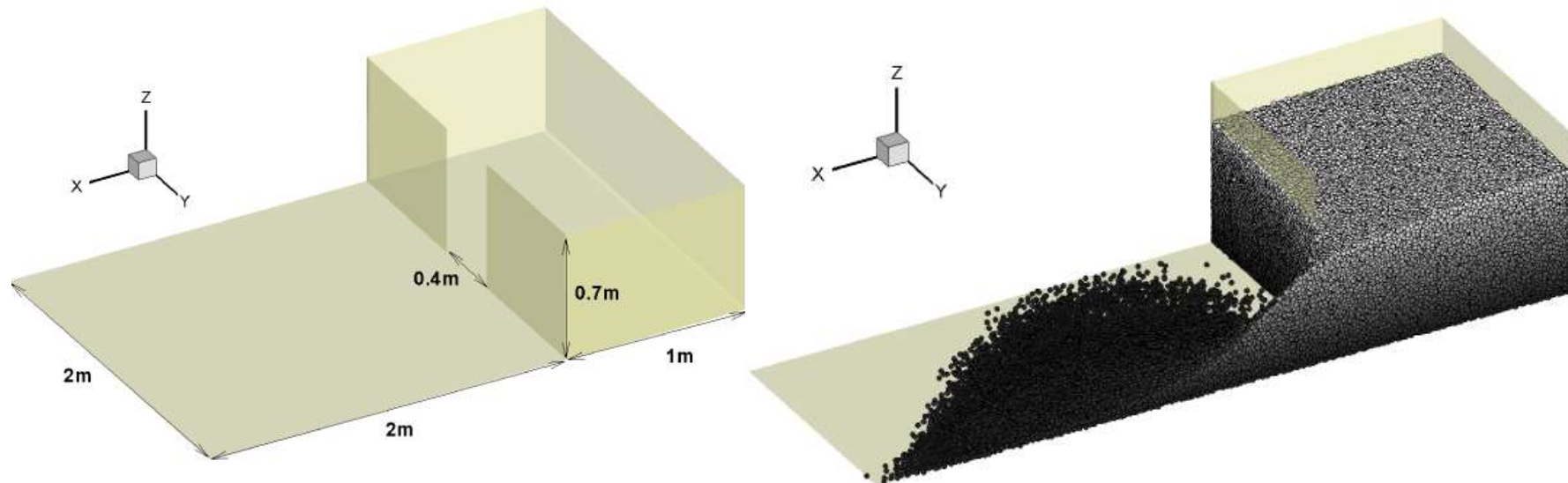
**Time t = 3.5 s**

$$\mu_N = 50 \text{ Pa} \cdot \text{s}$$



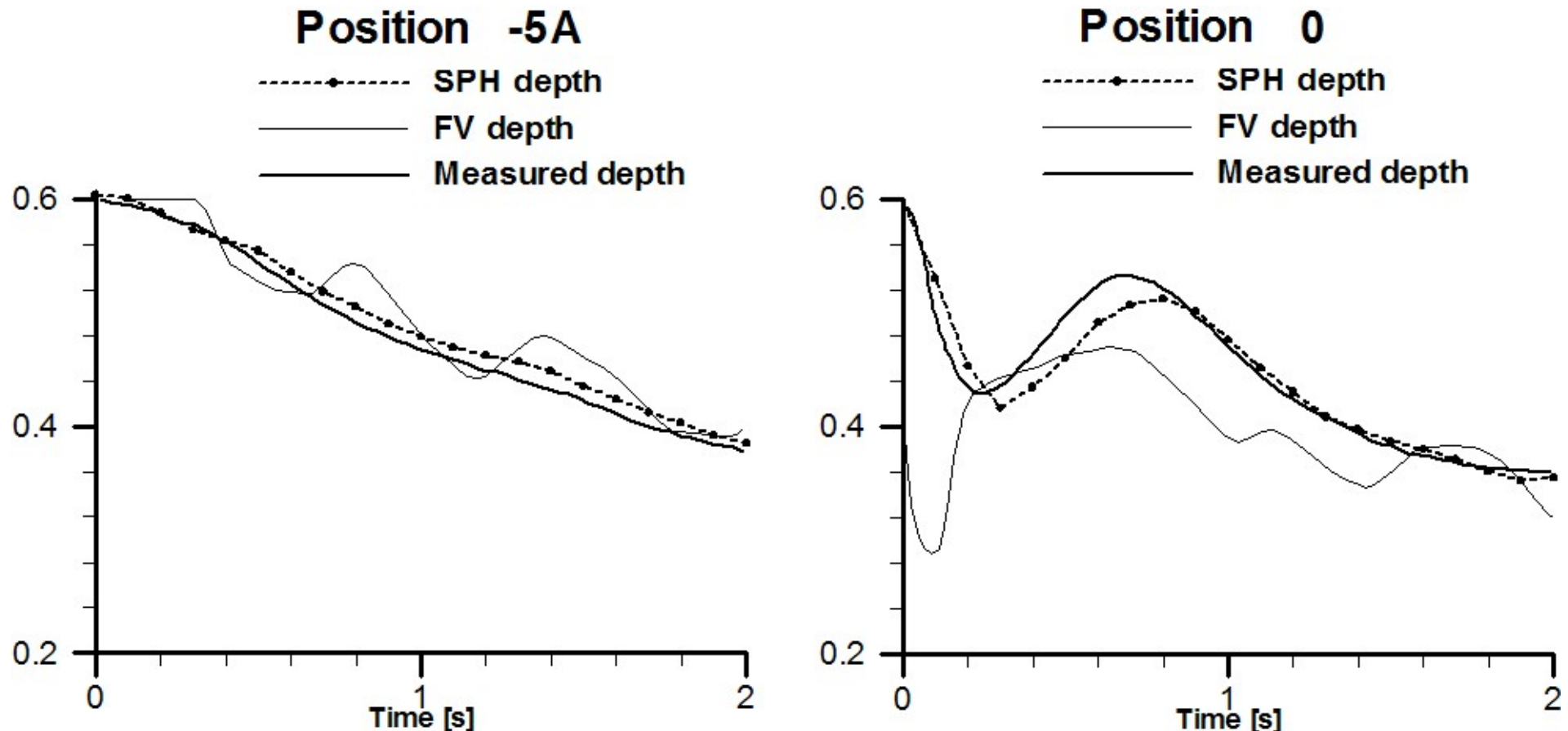
# Applications

The three-dimensional evolution flow after a dam break type problem.



# Applications

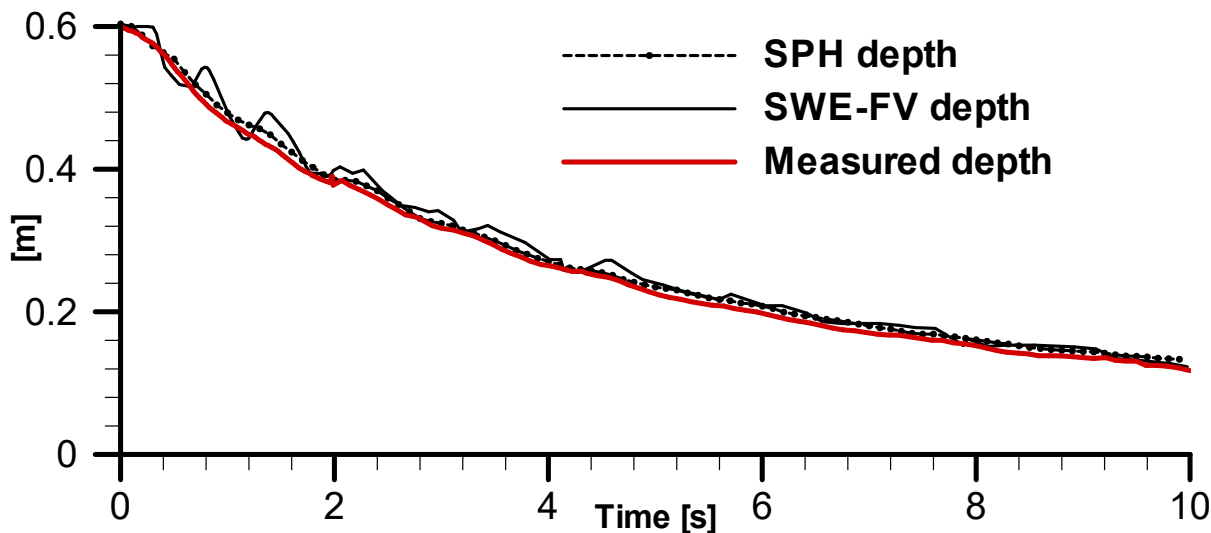
The three-dimensional evolution flow after a dam break type problem.



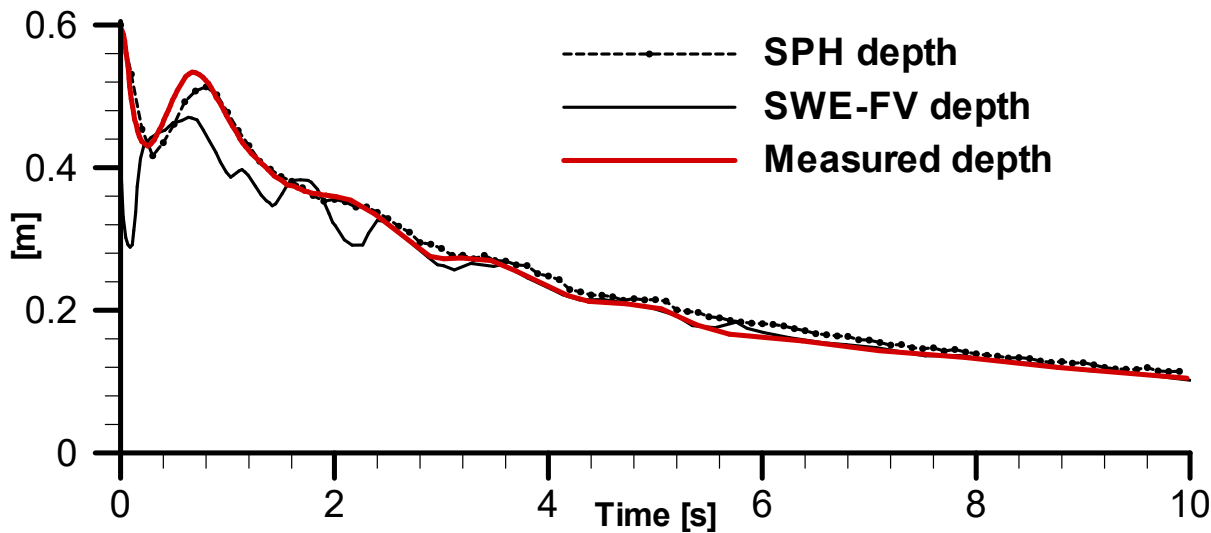
Fraccarollo, L. and Toro, E.F. (1995) J. of Hydraulic Research, 33,6:843-864.

# Applications

*Position -5A*

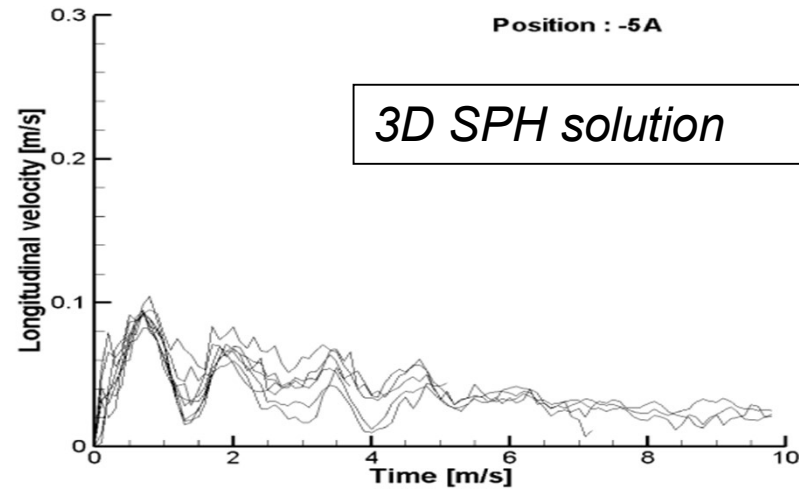
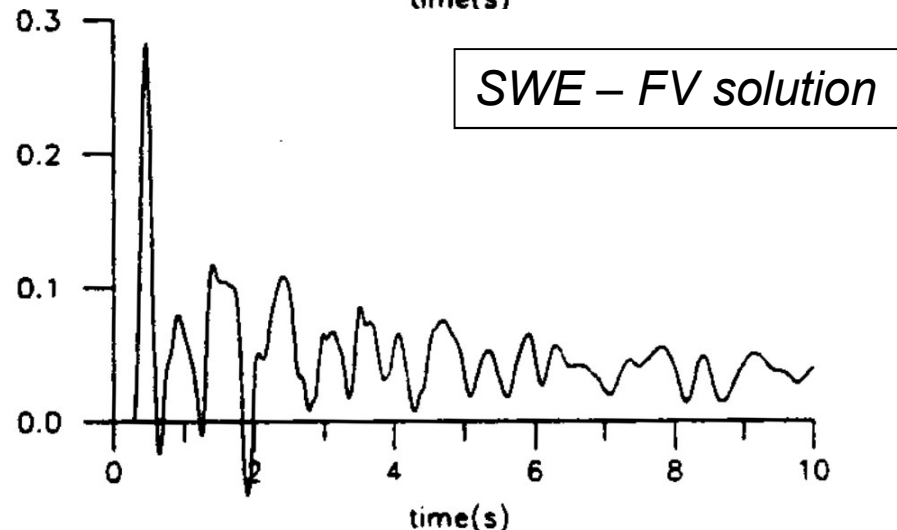
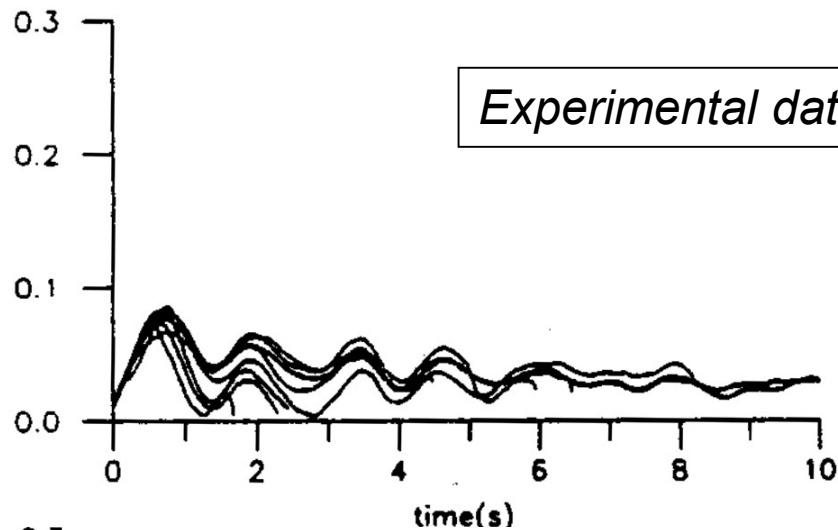


*Position 0*



Fraccarollo, L. and Toro, E.F. (1995) J. of Hydraulic Research, 33,6:843-864.

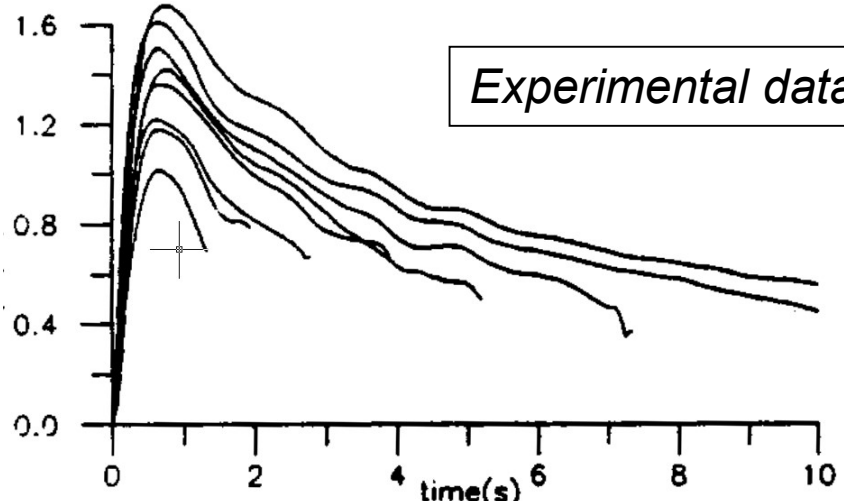
# Applications



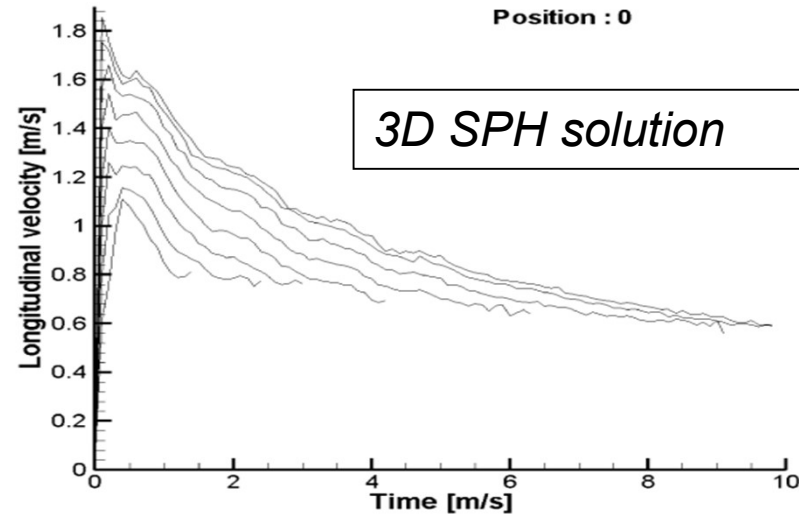
*Longitudinal component of the velocity at position -5A.*

Fraccarollo, L. and Toro, E.F. (1995) J. of Hydraulic Research, 33,6:843-864.

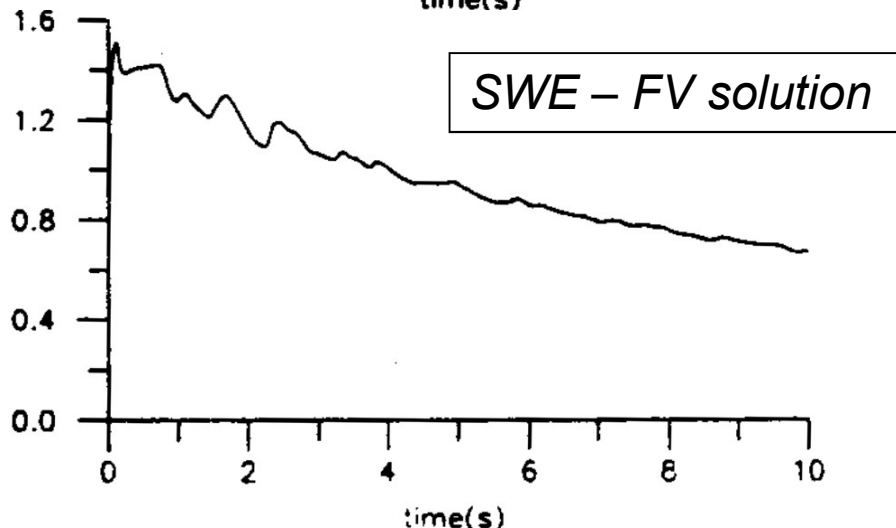
# Applications



*Experimental data*



*3D SPH solution*



*SWE - FV solution*

*Longitudinal component of the velocity at position 0.*

Fraccarollo, L. and Toro, E.F. (1995) J. of Hydraulic Research, 33,6:843-864.

# Applications

The test case consists of a *real* dam break problem happened in 1985 that produced a catastrophic *mudflow* on the village of Stava, in Trentino, Italy.



PhD. A. Ferrari



A new 3D parallel SPH scheme for free surface flows

2008

# Applications

The test case consists of a *real* dam break problem happened in 1985 that produced a catastrophic *mudflow* on the village of Stava, in Trentino, Italy.

Initial conditions:

$$\begin{cases} \mu_0 = 10^{-2} \text{ Pa}\cdot\text{s} \\ n = 1. \\ \tau_c = 0. \end{cases}$$

*The initial fluid particle spacing is 2 m.*

➡ The fluid in the tanks is discretized using **300'000 particles**.

*The particle spacing for the boundaries is 3 m.*

*60 s of simulation:*

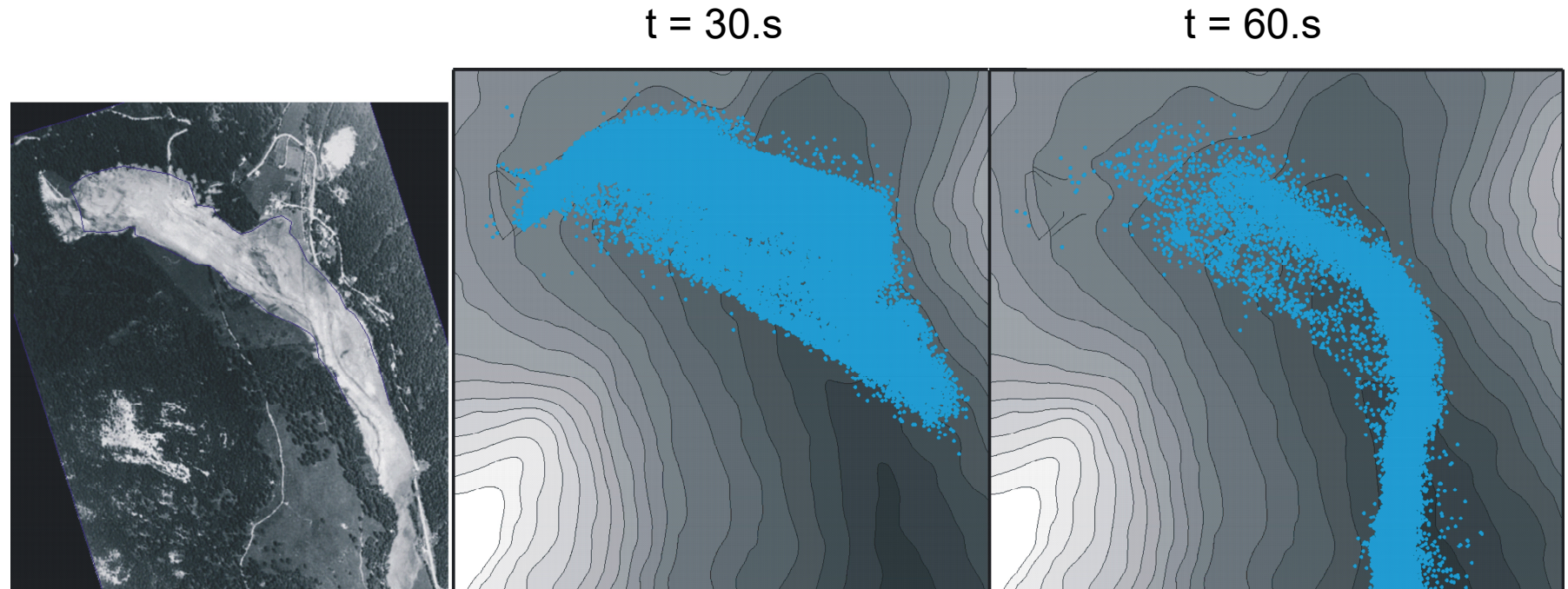
Videoclip

[Stava.avi](#)

# Applications

The test case consists of a *happened* (1985) dam break problem that has produced a catastrophic *mudflow* on the village of Stava, in Trentino, Italy.

Comparison between the real event and the numerical solutions

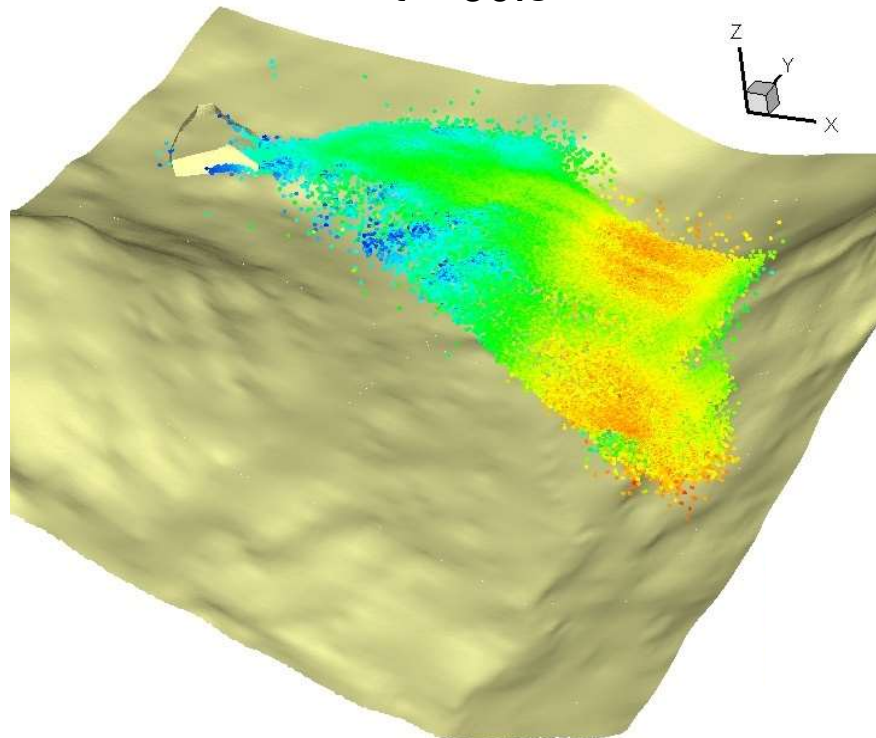


# Applications

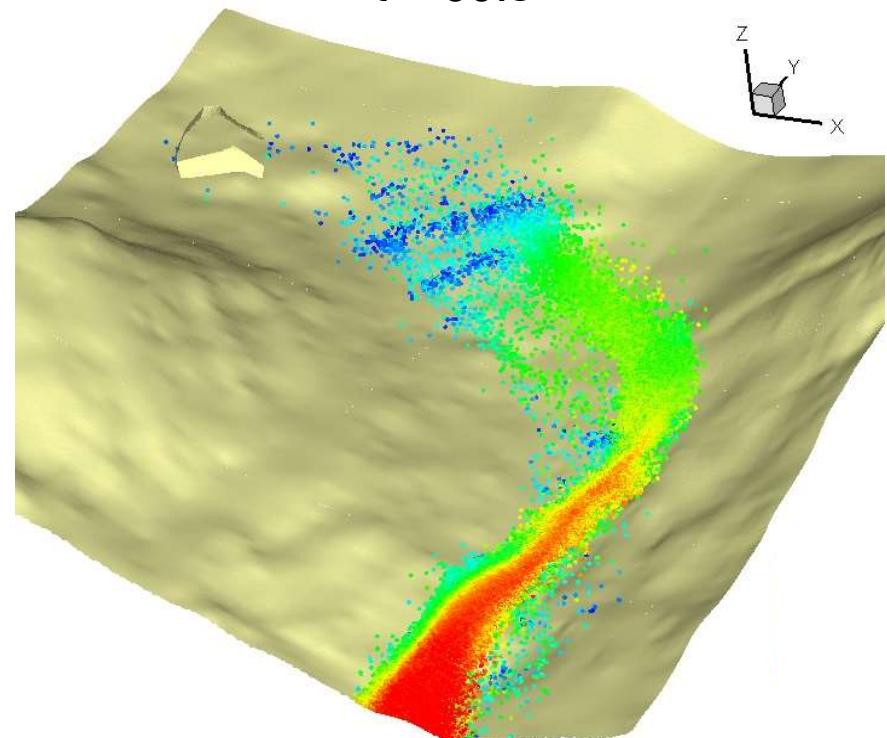
The test case consists of a *happened* (1985) dam break problem that has produced a catastrophic *mudflow* on the village of Stava, in Trentino, Italy.

Velocity field

$t = 30.s$



$t = 60.s$



## List of References, and references therein...

- [1] J.J. Monaghan, **Simulating free surface flows with SPH**, *J. Comput. Phys.* 110:399–406, 1994.
- [2] J. J. Monaghan, **Smoothed particle hydrodynamics**, *Rep. Prog. Phys.* 68(8):1703, 2005.
- [3] A. Ferrari, M. Dumbser, E.F. Toro and A. Armanini. **A New Stable SPH Scheme in Lagrangian Coordinates**, *Communications in Computational Physics*, 4(2):378-404, 2008.
- [4] A. Ferrari, M. Dumbser, E.F. Toro and A. Armanini. **A New 3D Parallel SPH scheme for Free Surface Flows**. *Computers & Fluids*, 38(6):1203-1217, 2009.
- [5] A. Ferrari, L. Fraccarollo, M. Dumbser, E.F. Toro and A. Armanini. **Three-Dimensional Flow Evolution after a Dambreak**. *Journal of Fluid Mechanics*, 663:456-477, 2010.
- [6] A. Ferrari. **SPH simulation of free surface flow over a sharp-crested weir**. *Advances in Water Resources*, 33:270-276, 2010.
- [7] D. Avesani, M. Dumbser and A. Bellin. **A new class of Moving-Least-Squares WENO–SPH schemes**, *Journal of Computational Physics*, 270:278-299, 2014